problems. Base on these, it could accelerate development of optimization theory of network planning and advance level of project management effectively.

"The maximal advantage of the algorithm used to find the shrink-critical path is that the least duration path which found out from whole network. It means that the effect that optimizing in whole could be realized by optimizing in local could be achieved by using the algorithm, and the workload of calculation could be reduced greatly. As the orientation of study in future, we should improve the algorithm to make it be more feasible".

The base of the algorithm is total float theorem not only is the theorem very important to resolve the problem of finding the shrink-critical path, but also the base of studying other relevant problems, and provide new theory and idea to study network planning. Seeing from point of development, the theorem and algorithm in this paper have important significance.

REFERENCES

[1] Jianxun Qi, Xiuhua Zhao "Hypo-Critical Path in Network Planning" Published by North China Electric Power University, *NCEPU*, Beijing, china. Vol 24 (2012) 1520-1529.

[2] S.E. Elmaghraby, "On Criticality and Sensitivity in Activity Networks", *European Journal of Operation Research*, Vol 127, pp. 220-238, 2000.

[3] J.E. Kelley and M.R. Walker, "Critical Path Planning and Scheduling", In; Proceedings of the *Eastern Joint Computational Conference*, vol. 16, pp. 160-172,1959.

[4] C.L. Liu and H.Y. Chen, "Critical Path for an Interval Project Networks", *Journal of Management Sciences in China*, Vol.9, no.1, pp. 27-32, 2006.

[5] S.H.An, P.R. Jie and G.G.He, "Comprehensive Importance Measurement for Nodes within a Node-Weighted Network", *Journal of Management Sciences in China*, vol.9, no.6,pp. 37-42, 2006.

[6] S.E. Elmaghraby, Activity Networks: Project Planning and Control by Network Models, NewYork: John Wiley & Sons Inc., 1977.

[7] J.X.Qi, New Theory of Network Planning and Technical Economics Decision-making, Beijing: Science Press,1997.

[8] S.E. Elmaghraby, "Activity Nets: a Guided Tour through Some Recent Developments", *European Journal of Operational Research*, vol. 82, pp. 383-408, 1995.

[9] X.M. Li and J.X. Qi, "Study on Time-Scaled Network Diagram Based on the Analysis of Activity Floats", *Operations Research and Management Science*, vol. 15, no. 6, pp. 28-33, 2006.

[10] X.M. Li, J.X. Qi and Z.X.Su, " The Research Resource Leveling Based on the Analysis of Activity Floats", *Chinese Journal of Management Science*, vol. 15, no. 1, pp. 47-54, 2007.

[11] D.J. Michael, J Kamburowski, "On Minimum Dummy Arc Problem", Operation Research, vol.27, no. 2, pp. 153-168, 1993.

[12] E. L. Demeulemeester and W. S. Herrelen, Project Scheduling, Boston: Kluwer Academic Publishers, 2002.

[13] S.E. Elmaghraby and Kamburowski, "On Project Representation and Activity floats", *Arabian Journal Of Science and Engineering*, vol.15, pp. 627-637,1990.

[14] S.H. Wang, X.S. Zhu and J.Li, "Research of A Step-by-Step CPM Base on Resource-Constrained", *Journal of Industrial Engineering and Engineering Management*, vol. 20, no.1, pp. 109-11, 2006.

[15] Y.C. Zhou, Y. P. Niu and B.L. Xiao et al, "Compute and Vision Secondary Critical Path Quickly in CPM Network", *Techno economics & Management Research*, vol. 2, pp. 61-62, 2004.

[16] J.W.Zhang, Y. Xu and Z. G.He et al, "A Review on the Time/Cost Trade-Offs Problem in Project Scheduling", *Journal of Industrial Engineering and Engineering Management*, vol.1, no. 21, pp. 92-97, 2007.

[17] X.Y. Zhang, and Z.W. He, "Discrete Time/Cost Trade-Offsin Project Scheduling with Time-sxitch Constraints ", *Chinese Journal of Management Science*, vol. 2, no. 14, pp. 58-64, 2006.

[18] X.L.Wu and Z.Yi, "Solving Time-Cost Trade-off Model for Activity Network by Minimum Cost Flow Principle", *Journal of Huazhong University of Science and Technology* (Nature Science Edition), vol. 1, no. 35, pp. 42-45, 2007.

[19] J. Li, Y. Shi and J. Y. Zhao, "Time-Cost Trade-off in a Transportation Problem with Multi-Constraint Levels", Or Transactions, vol. 5, no. 3, pp. 11-20, 2001.

[20] J.X.Qi, "The Theory of Loose Network and Group-Cut in the Optimization of Time-Cost", *Journal of System Engineering*, vol. 10, no. 1, pp. 113-126, 1995.

Modelling the resistance spot welding of galvanized steel sheets using Fuzzy logic controller

L. Boriwal
Research scholar, Mechanical Engineering Department, MANIT, Bhopal, India

R. M. Sarviya
Professor, Mechanical Engineering Department, MANIT, Bhopal, India

M. M. Mahapatra
Associate professor, Mechanical & Industrial Engineering Department, I. I. T, Roorkee, India

Abstract- The paper present the fuzzy logic based simulation for the resistance spot welding process, which is capable to predict the nugget size, tensile shear strength, and peel strength. Welding current, weld cycle and electrode pressure are taken as the process variables for RSW process. The experimental data were used for construction a fuzzy logic model to predict the effect of the input variables on the responses. The fuzzy model was also tested for a number of test cases to establish its adequacy. The error in predicting the outputs for the input data was within acceptable limits indicating the adequacy of the model to be used for complex processes like RSW.

Keywords: RSW welding, Fuzzy Logic Controller, Nugget size, tensile shear strength, tensile peel strength.

I. INTRODUCTION

Resistance spot welding (RSW) is one of the widely used joining processes in sheet metal fabrication and auto mobile industries. There are thousands of spot welds on an automobile body, so RWS is an important process in auto mobile industries [1]. The metal sheets intended to be welded using RSW are held together by the electrode pressure and current of very high magnitude (often in kA) is applied. The weld produced by an RSW process is commonly known as the nugget. The effect of electrical resistance on nugget formation with respect to the process variables has been studied [2]. The coating of steels can pose a problem during RSW especially if the coating material has a lower melting temperature and thus melts and vaporizes before the welding of the steel sheets can occur. Hence, coated steels such as galvanized steels need to be welded with care using appropriate process variables in order to prevent excessive degradation of the electrodes and defective welds. The characteristics of electrode radial wear and axial wear were compared with between DP600 and uncoated steels [3-4]. The quality of spot welds generally is checked by either destructive or non-destructive methods. The strength of the spot welded joints is usually determined by the tension shear and tension tests, that used here being the shear tension test. Fuzzy logic modelling method is one of the artificial intelligence (Al) techniques which have been in use for the modelling of manufacturing process such as machining and welding [5-6].The fuzzy logic model had developed for select drilling speeds for different material. [7]. Decision-making fuzzy control and Stability analysis of fuzzy systems are proposed in [8]. General treatments of fuzzy set theory, fuzzy logic, and fuzzy systems can be found in several [9]. Rule base fuzzy inference system had developed to study the hardness of sintered high speed steel [10]. No studies have been carried out on the fuzzy rule base inference system for predict the RSW response. Theory of fuzzy sets was proposed by L. A. Zadeh in 1965 [11]. Fuzzy logic is one of the artificial intelligence techniques. It is applicable in different area of science and engineering.

The aim of this study is construct rule base fuzzy logic model for predict the RSW response (Nugget size, Tensile shear strength and Tensile peel strength) with respect to process parameters such as welding current, weld cycle and electrode pressure.

II. FUZZY MODEL

Fuzzy system structure has four modules as show in fig.6. A fuzzifier that convert crisp input in to fuzzy value. Linguistic variables are defined as the variables whose values are sentences in natural language (such as low,

medium and high) and can be represented by fuzzy sets [14]. The structure of three inputs, three outputs fuzzy logic controller developed for present research.

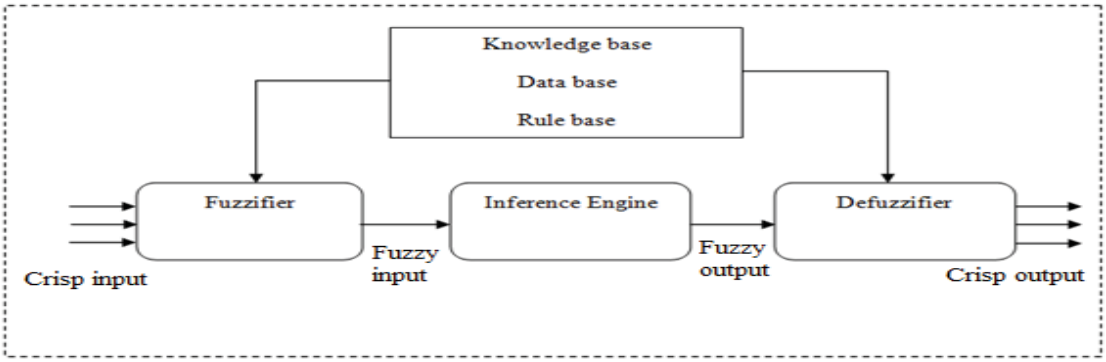

Fig. 6 General structure of fuzzy logic control system

Fuzzy logic controller use mamdani approach and contained a rule base model. This rule base comprised of groups of rules and each output was defined by 27 rules. Hence total numbers of rules for the three outputs such as nugget size, tensile shear strength and peel strength were 81. Table no. show the rule based on knowledge to predict the three output variables. The fuzzy rule base consists of a group of if–then control rules with the three input variables and three output variables that is:

Rule 1: if x_1 is A_1 and x_2 is B_1 and x_3 is C_1 then y is O_1 else
Rule 2: if x_1 is A_1 and x_2 is B_1 and x_3 is C_1 then y is O_2 else
Rule 2: if x_1 is A_1 and x_2 is B_1 and x_3 is C_1 then y is O_3 else

Rule n: if x_1 is A_n and x_2 is B_n and x_3 is c_3 then y is C_n.

Where x_1, x_2 and x_3 are fuzzy input variables and O_1, O_2 and O_3 are fuzzy labels of fuzzy set (Low, Medium and High). The triangular membership function is linear, was used for three input variables such as welding current, weld cycle, electrode pressure to predict the RSW output variable nugget size, tensile shear strength and peel strength. The membership function for all inputs variables were divided in the three levels (Low, Medium, and High) which is shown in Fig.8 .

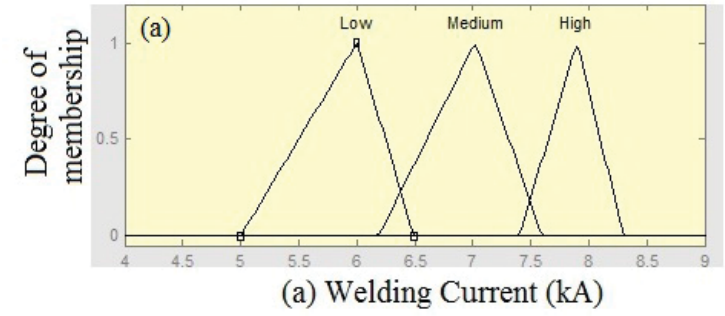

(a) Welding Current (kA)

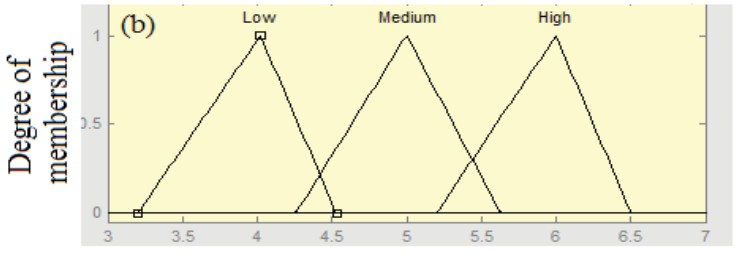

(b) Weld Cycle

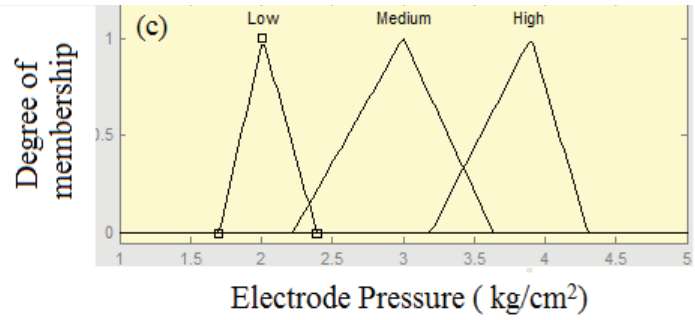

Fig.8 Membership function for input process parameters: (a) Welding current; (b) Weld cycle; & (c) Electrode pressure

In this paper, the fuzzy logic model was simulated for test cases which have been made between the fuzzy set ranges. The experiments were conducted for 3 levels of process variables such as welding current (6, 7.11 & 7.9 ampere), Weld cycle (4, 5 & 6) and electrode pressure (2, 3 & 4 kg/cm^2). The fuzzy logic model has been developed based on 27 experiments of RSW process variables. A MATLAB, Simulink model was prepared to call the output variables of RSW. The model developed was verified with a set of 12 input data for observing the predicted turnout. The predicted output of the model to test case data was further compared with the experimental output. The maximum percentage of error for prediction for peel strength was observed to be 17.44. The developed fuzzy logic model has been validated by the experiments and test case of resistance spot welding of steel sheet. Detail of the experiments is given below.

III. Experiment and Result

The test set for this evaluation experiment watermark image randomly selected from the internet. Matlab 7.0 The resistance spot welding was carried out using a constant-alternating current resistance welding machine. In the literature it is observed that electrode wearing occurred during the resistance welding of galvanized steel sheets. Because of zinc having a low melting temperature which results in it evaporating thereby affecting the surface quality of the electrode. Also, zinc fumes spoil the boundaries of the electrode tip. Each spot welding gives rise to the possibility of electrode wear. Hence the electrode diameter was checked each time before start welding operation. The electrode was ground, cleaned of scales and made to the desired diameter before each welding. A set of electrodes were kept ready with similar diameter to be used for welding. A schematic of the process and machine used and used for the experiment is shown in Figure 1. The electrode was cooled by circulating water during the entire period of the welding process. The thickness of the galvanized steel sheet used in the experiments was 0.8mm. The specimens were prepared with 100 X 30X 0.8 mm in size as shown in Figure 2. Sheet surfaces were cleaned with a dry air jet before RSW. Trial runs were initially conducted for spot weld to set the levels of three welding input process parameters such as welding current, weld cycle and electrode pressure. These parameters were set in the microcomputer for welding. Overlapped sheets (by 30 mm, Figure 2) were placed between the two electrodes centre which was marked on the specimens to set the electrode face for producing spot welds at the centre.

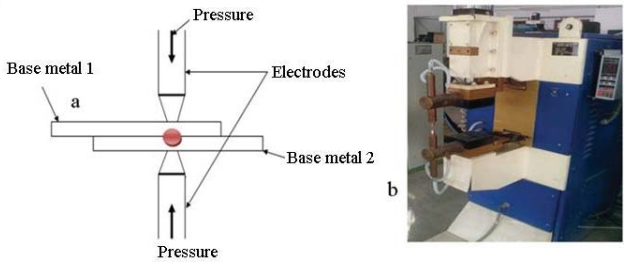

Fig. 1 Schematic view of (a) the process, (b) the machine

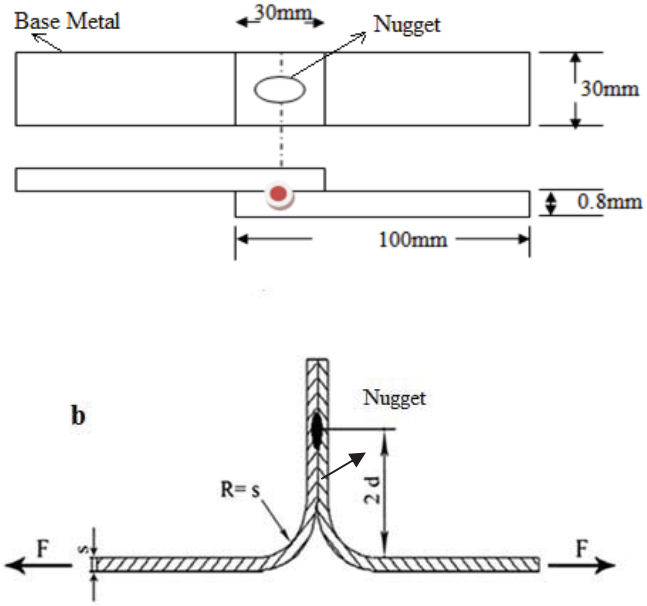

Fig. 2 Schematic illustration of a weld specimen

The chemical composition of the galvanized steel sheet material is given in Table 1. The schematics of the specimens used for testing strength are shown in Figure 2. Copper alloy was as the electrode material in the experiments. Chemical composition of the electrode material is shown in Table 2. Experiments were conducted for 27 test samples to obtain data for building the fuzzy logic model. Test case study of galvanized steel sheet was done with same experimental procedure expect the values of process parameters used in the design matrix. Process parameters for the test cases are shown in Table 4.

Table 1 Chemical composition (%) of steel sheet used in experiment

C	Mn	S	P	Si	Cr	Ni	Mo	Cu	Nb	Fe
0.115	0.39	0.017	0.018	0.065	0.017	0.032	0.004	0.051	0.001	Base

Table 2 Chemical composition of electrode used in experiment

Al	Mg	Cu%	Si	P
0.6353	0.0768	99.065	0.1954	0.0272

Table 4 Process parameter for test case

Sl. No	Welding current (kA)	Welding cycle	Electrode pressure (kg/cm^2)
1	6.66	4	2.6
2	6.66	5	3.2
3	6.66	5	3.4
4	6.66	5	3.6
5	6.66	6	3.6
6	7.02	4	2.6
7	7.02	4	2.8

8	7.02	5	2.8
9	7.02	5	3.2
10	7.02	6	3.6
11	7.8	4	3.6
12	7.8	5	3.6
13	7.8	6	3.6

Table 5 Predicted and measured values of the outputs in the test cases

	Nugget size (mm)			Tensile shear strength (kN)			Tensile peel strength (kN)		
Sl. No	Measured (mm)	Predicted (mm)	Error (%)	Measured (kN)	Predicted (kN)	Error %	Measured (kN)	Predicted (kN)	Error %
1	1.95	1.815	6.923	2.6	2.262	13	1.37	1.311	17.44
2	3.09	3.436	11.197	3.8	3.532	7.052	1.88	1.664	11.489
3	3.1	3.452	11.354	3.6	3.494	2.944	1.75	1.655	5.428
4	2.92	3.416	16.986	3.3	3.412	3.393	1.65	1.612	2.303
5	3.89	3.436	2.234	4.52	4.583	1.39	2.128	2.278	7.048
6	1.88	1.834	2.446	2.2	2.267	3.045	1.09	1.121	2.844
7	1.76	1.83	3.977	2.15	2.2	2.325	1.075	1.122	4.372
8	3.01	3.324	10.43	3.25	3.55	9.23	1.6	1.659	3.687
9	2.89	3.2	10.72	4	3.54	11.5	1.9	1.668	12.21
10	3.68	3.435	6.657	4.1	4.582	11.756	2.09	2.275	8.851
11	3.58	3.431	4.162	3.3	3.433	4.03	1.52	1.664	9.473
12	3.89	3.542	8.946	3.9	3.533	9.41	1.95	1.754	10.051
13	4.5	4.77	6	4.42	4.582	3.665	2.19	2.278	4.018

IV.CONCLUSION

An Fuzzy logic model was developed for the RSW process and the developed model was used to predict the nugget Size, tensile strength and peel strength in terms of the three inputs welding current, weld cycle and electrode pressure of RSW process. In this research RSW outputs (Nugget size, tensile shear strength and Peel strength) have been successfully predicted for full factorial design experimental data and for test case. The developed fuzzy model was also tested for a number of test cases, the input data of which was not used in the building the fuzzy logic model. The error in predicting the outputs for the input data was within acceptable limits indicating the adequacy of the model to be used for complex processes like RSW.

REFERENCES

[1] Fundamentals of American *Welding Society*. Welding Handbook Volume 1,1980

[2] American Welding Society. *Welding Handbook* Volume 3,1980

[3] Holliday, R., Parker, J. D. and Williams, N. T. Electrode deformation when spot welding coated steels. *Weld. in the World*, 35(3), 160-164,1995

[4] Na, S. J. and Park, S.W. A theoretical study on electrical and thermal response in resistance spot welding, *Welding Journal*., 8, 233s–41s,1996

[5] Pouranvari M., Marashi S.P.H., Key factors influencing mechanical performance of dual phase steel resistance spot welds, *Sci Technol Weld Join*, Vol. 15, pp.149-155,2010

[6] Sun X., Stephens E. V., Davies R. W., Khaleel M. A., Spinella D. J., Effects of Failure Modes on Strength of Aluminum Resistance Spot Welds, *Welding Journal*, Vol. 83, pp.188s–195s,2004

[7] Deng X., Chen W., Shi G., Three-dimensional finite element analysis of the mechanical behavior of spot welds, *Finite element in analysis and design*, Vol. 35, pp. 17-39,2004

[8] M. Zhou, A unified approach to assessing the mechanical performance of resistance spot welds, PhD Dissertation, University of Michigan, An Arbor, MI, 2003

[9] Zhang H., Zhou M., Hu S. J., "Impact Strength Measurementof Spot Welds ", *Proceedings of the institution of Mechanical Engineering, Part B: Journal of Engineering Manufacture*, Vol. 215, pp.403-414, 2001

[10] Nieto1 J., Guerrero-Mata M. P. Colas R., Mani A,Experimental investigation on resistance spot welding of galvannealed HSLA steel, *Sci. Technol. Weld. Joining*, Vol. 11, pp. 717-722,2006

[11] Gould J. E., Khurana S. P. and Li T., Prediction of microstructure when welding automotive advanced high – strength steels, *Welding Journal* Vol. 86, pp. 111s – 116s,2006

[12] Long , Dr. Khanna S. K., "Finite element analysis of residual stress generation during spot welding and its effect on fatigue behaviour of spot welded joint" , PhD thesis, University of Missouri- Columbia, 2005

[13] Donders S., et al., Effect of spot weld failure on Dynamic Vehicle Performance, Report (http://www.caeda.com.cn/materials/solution/2005IMAC_spot weldFailure. pdf)

[14] Badheka V. J., Agrawal S. K. and Shroff N., " Resistance spot welding of martensitic Stainless Steel (SS420) Part – I" IJMME, Vol. 3, 328-340, 2009

Real Power Allocation in Open Access Environment

Debdeep Saha
Girijananda Chowdhury Institute of Management and Technology

Dr. Sarmila Patra
Assam Engineering College

Abstract— Tracing the flow of electricity becomes an important issue under transmission open access. In practice, power flow follows the physical laws of electricity and therefore it is not straight forward to map out how the participants make use of the system. This article focuses on presenting an analysis of the performance of major power tracing methods based on proportional sharing principle namely the Graph Theory. The power transmission costs, which are charged to the market participants, are a central issue of the new deregulated electricity markets. The article implements a methodology for transmission cost allocation based on the principle of proportional sharing states that any power flow leaving a bus is made up of the flows entering that bus in a proportional manner, thus satisfying Kirchhoff first law. To carry out the computer tests, IEEE 6 and 30 bus systems are taken to allocate real power as a part of transmission loss allocation. It also allows the assessment of contributions of individual generators (or load) to individual line flows.

Index Terms— Transmission loss allocation, Graph theory, deregulation, monopolistic.

I. INTRODUCTION

Transmission loss allocation is the process of assigning to each individual generation and load the responsibility of paying for a part of the system transmission losses. Although no power system variable is affected by this process, the revenue and payment reconciliation are dependent on the criterion adopted for this purpose Transmission loss allocation is not an easy task. Even in a simple two-node system with one generator supplying a single load, loss allocation between the generator and the load has to be agreed upon as there is no physical measurement or mathematical method that determines the loss shares in a unique manner. In a real system, matters obtain more complicated because of two facts. The first is that the determination of the line flows caused by each load through each transmission line has a good degree of arbitrariness. The second is that the transmission line loss is a nonlinear function of the line flow, and hence cannot be separated between partial flows through the same line in a unique convincing way [3]. Continuing trend towards deregulation and unbundling of transmission services has resulted in the need to assess what the impact of a particular generator or load is on the power system. A new method of tracing the flow of electricity in meshed electrical networks is proposed which may be applied to both real and reactive power flows. The method allows assessment of how much of the real and reactive power output from a particular station goes to a particular load. It also allows the assessment of contributions of individual generators (or load) to individual line flows [6].

In a competitive environment, usage allocation questions must be answered clearly and unequivocally. To help answer such questions, this article practices a proposed method for determining how much of the active and reactive power output of each generator is contributed by each load. This method takes as its starting point a solved power flow solution. Having determined where the power goes, one can compute how much power flows from a given generator to each load or from all generators to a particular load. It is also possible to determine how many MWs each load or generator contributes to the active flow in a branch. These physical "contributions" form a basis upon which the cost of building and maintaining each component of the network could be allocated among its users Computation of the contributions defined and used in is possible only if the quantities being allocated are linearly additive. This implies that active and reactive powers should be considered separately. Power flows of generators and loads are traced to determine the transmission system usage by each generator and load. Then, transmission losses caused by each generator or load are determined. Based on power flow tracing methodology, topological generation and load distribution factors are determined in through matrix inversion, with additional nodes added to represent line losses.

II. POWER TRACING

The monopolistic, vertically integrated power system has now become market driven. In this new operating environment, determining the impact of individual market players on the system has become very significant. To ensure fair competition among the players, all financial transactions should be transparent, and none of the costs should be allowed to be subsidized or cross-subsidized. In such a structure a transmission system is being used by multiple generation and load entities that do not own the transmission system. In view of market operation it becomes more important to know the role of individual generators and loads to transmission wires and power transfer between individual generators to loads. Transparency can be accomplished only when the power-flow path of a generator and its flow extent are known. This information, which can be determined by power-flow tracing, not only enables the independent system operators (ISOs) to pay proper revenue to the generators, but it also proves to be a very important tool for different analytical purposes [8].

Usage allocation refers to power contribution of each generator to each load. The advantage of knowing the usage allocation includes loss allocation associated to each path, cost assignment to transmission line pricing, congestion management, ancillary services and decision on scheduling of generators. To achieve the above mentioned advantages several schemes have been developed to solve the allocation problem. Methods based on dc load flow and sensitivity analysis cannot consider accurately, the reactive power transfer allocation and system non linearity. The bilateral transaction approach aims at assigning the transmission cost of any specific transaction between two nodes. Research has been carried out by unbundling the flow of electricity based on individual transactions taking place which is theoretically very difficult. Other commonly used approaches include application of superposition theorem and power tracing methods.

The proportional sharing principle basically amounts to assuming that the network node is a perfect 'mixer' of incoming flows so that it is impossible to tell which particular inflowing electron goes into which particular outgoing line. This seems to agree with common sense and with the generally accepted view that electricity is indistinguishable. The concept of "power flow tracing" between generators and transmission has been discussed for determining wheeling rates of new users under deregulated environments [6].

III. FUNDAMENTALS OF LOAD FLOW TRACING

In order to simplify the problem, we first make the following basic assumptions:

a) An ac load flow solution is available from on-line

state estimation or off-line system analysis. The studied system has finite number of buses. It is operated properly and there is no loop flow in the system.

b) Real power and reactive power required by

Transmission line resistance, reactance and charging capacitance have been moved to the line terminal buses (see Section III for details) and modelled as "equivalent loads" according to ac load flow solution. Therefore the line active and reactive power flows keep constant along the line, each edge has a definite direction and the network is "lossless."

c) A generator has the priority to provide power to the

load on the same bus. The remaining power will enter the network to supply other loads in the network to avoid unnecessary losses. It is true even according to a transaction contract a generator does not sell electricity to the local load. This is because electricity has no label and system operators have the authority to dispatch the power flow. Therefore the buses of a network can be classified as generator buses, load buses and network buses based on their net injection to the system. This concept can be applied to both active and reactive power flows.

d) The flows of electricity obey the proportional-sharing

Rule.

The above assumption leads to the following lemmas-

Lemma 1: A lossless, finite-nodes power system without loop flow has at least one pure source, i.e. a generator bus with all incident lines carrying outflows. This lemma will be proved below. It guarantees to start and continue a downstream tracing from an existing pure source.

Lemma 2: A lossless, finite-nodes power system without loop flow has at least one pure sink, i.e. a load bus with all incident lines carrying inflows [8].

IV. PROPORTIONAL SHARING PRINCIPLE

The proportional sharing principle is based on Kirchhoff's current law. It deals with a general transportation problem and assumes that the network node is a perfect mixer of incoming flows. Practically the only requirement for the input data is that Kirchhoff's current law must be satisfied for all the nodes in the network. In this respect the method is equally applicable to ac as well as dc power flow. As electricity is indistinguishable and each of the outflows down the line from node i is dependent only on the voltage gradient and impedance of

the line, it may be assumed that each MW leaving the node contains the same proportion of the inflows as the total nodal flow P [6]. The nodal sum i.e. total incoming and total outgoing power at node is equal. The main principle used to trace the flow of electricity will be that of proportional sharing is shown in Fig 1(a). In this, four lines are connected to node **a,** with two inflows and with two with outflows. The total power flow through the node is Pa = 40 + 60 = l00MW of which 40% is supplied by line j-a and 60% by line k-a.

According to proportional sharing principle-

The 70MW outflowing in line a-m consists of

70*40/100=28 MW. supplied by line j-a and

70*60/100=42MW supplied by line k-a**.**

Similarly the 30MW outflowing in line a-n consists of

30*40/100=12MW supplied by line j-a and

30*60/100=18 MW supplied by line k-a.

The proportional sharing principle basically amounts to assuming that the network node is a perfect 'mixer' of incoming flows so that it is impossible to tell which particular in flowing electron goes into which particular outgoing line. The principle is fair as it treats all the incoming and out-flowing flows in the same way.

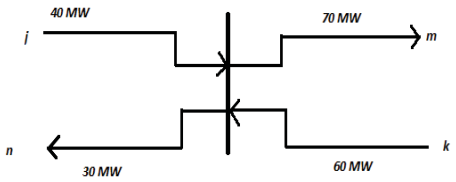

Fig 1(a): Representation of Proportional Sharing Principle

V. DOWNSTREAM LOOKING ALGORITHM

Now consider the dual, downstream-looking, problem when the nodal through-flow *P,* is expressed as the sum of outflows

$$P_i = \sum | P_{i-l} | + P_{Li}$$

$$P_i = \sum C_{li} P_i + P_{Li}$$

where alpha(i)^d is, as before, the set of nodes supplied directly from node i and

$$C_{li} = | P_{i-l} | / P_l$$

This equation can be rewritten as

$$P_i - \sum C_{li} P_i = P_{Li}$$

$$A_D P = P_L$$

Where A_d is the *(n* x *n)* downstream distribution matrix and P, is the vector of nodal demands. The (i.l) element of A_d is equal to

$$[A_d]_{il} = \begin{cases} 1 \\ -C_{li} = -| P_{i-l} | / P_l \\ 0 \end{cases}$$

Note that **A,** is also sparse and non symmetric. Adding and gives a symmetric matrix which has the same structure as the nodal. Admittance matrix. If A_d^{-1} exists then $P = A_d^{-1} P_L$ and its ith element is equal to

$$P_i = \sum [A_l^{-1}]_{ik} P_{ik} \quad \text{for i=1,2…..n}$$

This equation shows how the nodal power P, distributed between all the loads in the system. On the other hand, the same P_i is equal to the sum of the generation at node ***i*** and all the inflows in lines entering the node. Hence the inflow to node ***i*** from line **i-j** can be calculated using the proportional sharing principle as

$$| P_{i-l} | = (| P_{i-l} / P_i) P_i = (| P_{i-l} | / P_i) \sum [A_l^{-1}]_{ik} P_{ik}$$
$$= \sum D_{i=j}, k^L P_{LK}$$

Where $\sum D_{i=j}, k^L P_{LK}$ is the topological load distribution factor that is the portion of kth load demand that flows in line i-j.

This definition is again similar to that of the generalized load distribution factor based on DC load-flow sensitivity analysis. However, the topological factor represents the share (which is always positive) of the load in a line flow while the generalized factor determines the impact of the load on a line flow and may be negative. The generation at a node is also an inflow and can be calculated using the proportional sharing principle as

$$P_{Gi} = (P_{Gi} / P_i) P_i = (P_{Gi} / P_i) \sum [A_d^{-1}]_{ik} P_{ik}$$

This equation shows that the share of the output of the ith generator used to supply the kth load demand is equal to $P_{Gi} P_{LK} [A_d^{-1}]_{ik} / P_i$ and can be used to trace where the power of a particular generator goes to[6].

VI. RESULTS AND DISCUSSIONS

(A) An application with IEEE 6 bus system

To make the applied method easy to understand, a small test system was selected to explain the steps involved. The one-line diagram of the system is shown in Figure 7(a), and the system data can be found. From the power-flow results, the direction of power flows through the lines can be determined. The real power-flow direction is indicated by the arrows placed under the branches.

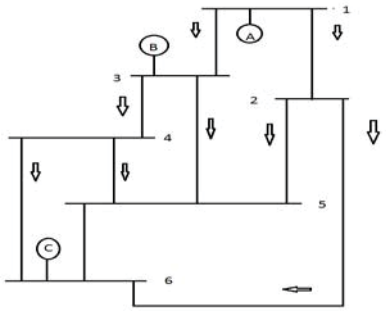

Fig2 (a): Single line diagram of 6 bus system

Three generators are connected to buses 1, 3, 6. From the power-flow directions shown in the figure, it can be seen that only bus 1 is the start buses, as the bus has all the outgoing power. All other generator buses, namely buses 3 and 6, do not get power only from the generators connected to that bus through the transmission lines. For instance, bus 3 gets power from bus 1, while. Again, bus 6 is only the bus where all of the connecting lines carry incoming power, and no line carries power out of this bus. So, bus 6 is the only end bus in this system. This process of selecting start and end buses should be repeated for reactive power flow also, as this might result into a different set of start and end buses. In this case, there will be a single start bus for reactive

power flow at bus 1.Once the start and end buses are selected, the flow direction matrix (F) is formed. Matrix F for active power allocation of the test system is shown below:

Table 1(a): Flow Incidence Matrix of 6 bus system

F =

	1	2	3	4	5	6
1	0	1	1	0	0	0
2	0	0	0	0	1	1
3	0	0	0	1	1	0
4	0	0	0	0	1	1
5	0	0	0	0	0	1
6	0	0	0	0	0	0

The elements of F having value 1 indicate a direct connection between the corresponding buses. As bus 1 is directly connected to bus 2 and 3 only, and the direction of the power flow is from bus 1 to bus 2, so the first row of F has a double 1 value in column 2 and 3. In bus 6, although there are three lines connected, power flow in all of these buses is toward this bus, so all of the elements in the last row of F are 0.
The total inflow for each of the buses is calculated, followed by the calculation of the contribution for each of the generator buses on itself. This is taken as 1 if the generator is a start generator. So, for the six-bus system, the contribution of generators 1 toward itself will be 1. For all other generators at buses 3 and 6, their contributions on the bus where they are connected will be calculated as

$$C_{33} = P_{G3} / P_3$$

where PG3 is the output of the generator at bus 3, and P3 is the total inflow at bus 3.

Once the contribution of generators toward their own buses are over, any of the start buses is selected (1, here), and the contribution of this bus is calculated for all the buses (j) having a non-zero element of F corresponding to this new bus. From the flow-direction matrix shown above, it is seen that, corresponding to bus 1, only bus 2 has a non-zero element. So, the contribution of bus 1 on bus 2 will be

$$C_{12} = P_{12} / P_2$$

where P12 is the power flow from bus 1 to bus 2, and P2 is the total inflow at bus 2. Bus 2 will now be considered as the start bus, and the process will be repeated for all other buses until it reaches any one of the end buses. These steps are repeated for all generators. The resulting contribution matrix, which gives the contribution of each bus

Table 1 (b): Contribution matrix

C =

	1	2	3	4	5	6
1	1	1	0.0909	0.0909	0.7413	0.6039
2	0	0	0	0	0.7143	0.4286
3	0	0	0.9091	0.9091	0.2597	0
4	0	0	0	0	0.1429	0.2143
5	0	0	0	0	0	0.2143
6	0	0	0	0	0	0.1429

If any bus has a contribution value of less than 1 toward itself (here buses 2, 3, 4, and 6), then its contribution for all other buses gets modified by multiplying each of the contribution value for that bus by its self-contribution, which is less than 1 (as per Step 11 of the algorithm). The final contribution matrix of the generators toward the active load for the test system is

Table1 (c): Final contribution Matrix

C =

	1	2	3	4	5	6
1	1	1	0.0909	0.0909	0.7413	0.6039
2	0	0	0	0	0	0
3	0	0	0.9091	0.9091	0.2597	0.2505
4	0	0	0	0	0	0
5	0	0	0	0	0	0
6	0	0	0	0	0	0.1429

The contribution of a generator toward a bus is considered to be same as the generator's contribution to all branches connected to that bus and having an outward power flow direction from the bus into the branch. So, determining the bus from which power is sent into the branch will lead to the contribution of generators on the branch loss as well as branch flow. Similarly, the contribution of any load on branch loss will be the same as the contribution of the load on the bus that is connected to the branch and carries power in an outward direction from the branch toward the load. The contribution of individual generators on the load is represented by the following graph-

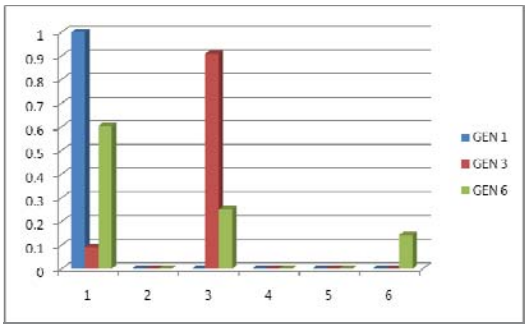

Fig 1(c): Graphical Representation of generator contribution to loa

From the figure, it is clear that

(i) Generator 1 is supplying 100% power to Bus 1.

(ii) Generator 3 is supplying 9.09% power to Bus 1 and 90.9% power to Bus3

(iii) Generator 6 is supplying 60.3% power to Bus 1, 25.05% power to Bus 3 and 14.29% power to Bus 6.

(B) An application with IEEE 30 bus system

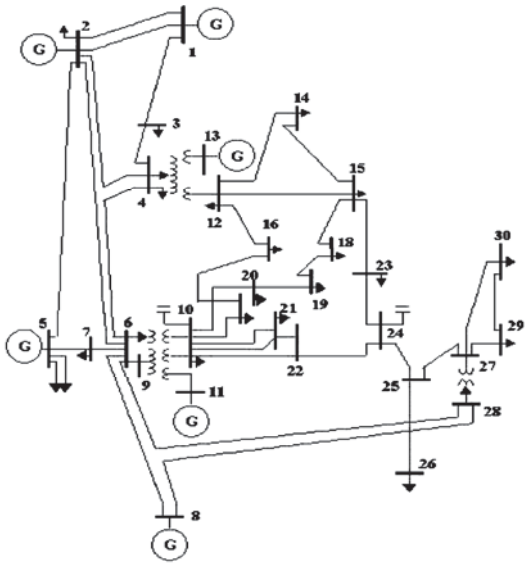

Fig 3(a): Single line diagram of 30 bus system

Considering bus 1 as the start bus, reactive power is traced in the above system. Starting with the flow-incidence matrix, the connections are checked between each lines are contribution is analyzed by proportional sharing principle.

Following the similar steps of Downstream Looking Algorithm, the above system is traced for reactive power and the updated contribution matrix is shown in Table 5

The contribution of individual generators on load buses can be represented as-

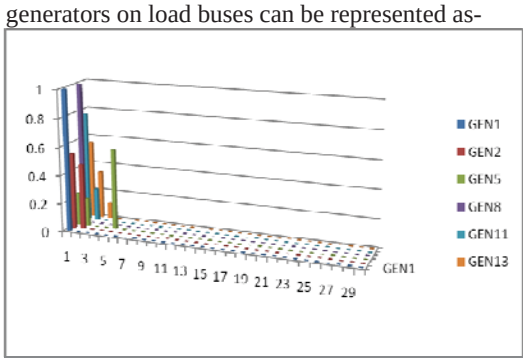

Fig 3 (b): Graphical representaion of contribution of individual generators to load

The final contribution matrix which shows the contribution of the 6 generators on the 30 individual buses is as follows-

Table 2(a): Final contribution matrix of 30 bus system on the 6 generators

	GEN1	GEN2	GEN5	GEN8	GEN11	GEN13
1	1	0.5356	0.2296	1	0.7729	0.5504
2	0	0.4644	0.1991	0	0.2271	0.3356
3	0	0	0	0	0	0.114
4	0	0	0	0	0	0
5	0	0	0.5713	0	0	0
6	0	0	0	0	0	0
7	0	0	0	0	0	0
8	0	0	0	0	0	0
9	0	0	0	0	0	0
10	0	0	0	0	0	0
11	0	0	0	0	0	0
12	0	0	0	0	0	0
13	0	0	0	0	0	0
14	0	0	0	0	0	0
15	0	0	0	0	0	0
16	0	0	0	0	0	0
17	0	0	0	0	0	0
18	0	0	0	0	0	0
19	0	0	0	0	0	0
20	0	0	0	0	0	0
21	0	0	0	0	0	0
22	0	0	0	0	0	0
23	0	0	0	0	0	0
24	0	0	0	0	0	0
25	0	0	0	0	0	0
26	0	0	0	0	0	0
27	0	0	0	0	0	0
28	0	0	0	0	0	0
29	0	0	0	0	0	0
30	0	0	0	0	0	0

VII. CONCLUSION

This Article uses a method for power-flow tracing and allocation of transmission losses based on the power-flow results. It employs the graph theoretic methods directly to determine the contribution of the generators to individual loads or line flows. Unlike other graph theory based approaches, the method does not require sub-grouping of the system buses. This makes the method very simple to implement, and also it significantly

decreases the computation time. The method allocates loads and losses to the generators avoiding any possibility of cross-subsidy. So, increased accuracy and improved speed with the very simple approach of the method are its main advantages over the other similar methods, considering the premium value of the power and energy losses.

REFERENCES

[1] Janusz bialek "Tracing the flow of electricity" IEE Proc.-Gener. Transm. Distrih., Vol. 143, No 4, July 1996

[2] Daniel Kirschen Ron Allan Goran Strbac "Contributions of Individual Generators to Loads and Flows "IEEE Transactions on Power Systems, Vol. 12, No. 1, February 1997.

[3] Ya-Chin Chang*, Chan-Nan Lu "An electricity tracing method with application to power loss allocation Electrical Power and Energy Systems 23 (2001) 13–17"

[4] C.-T. Su, J.-H. Liaw and C.-M. Li 'Power-flow tracing and wheeling costing considering complex power and convection lines' IEEE Proc.-Gener. Transm. Distrib., Vol. 153, No. 1, January 2006.

[5] M. W. Mustafa, Member, IEEE and H. Shareef, Student Member, IEEE "A Comparison of Electric Power Tracing Methods Used in Deregulated Power Systems." First International Power and Energy Conference PECon 2006 November 28-29, 2006, Putra.

[6] Sobhy M. Abdelkader," Transmission Loss Allocation Through Complex Power Flow Tracing" 2240 IEEE Transactions on power system, VOL. 22, NO. 4, November 2007.

[7] M.DE1 and S. K. GOSWAMI1." A Direct and Simplified Approach to Power-flow Tracing and Loss Allocation Using Graph Theory" Electric Power Components and Systems, 38:241–259, 2010

Weighted Clustering Algorithms in MANET: A Survey

Amit Gupta
Department of Computer Science and Engineering
UIT-RGPV, Bhopal, Madhya Pradesh, India

Abstract- A mobile adhoc network (MANET) is a collection of independent mobile nodes that communicate over relative bandwidth and power constrained wireless links. The network topology may transform quickly and randomly due to mobility of nodes. Also, in MANET the decentralized network leads to perform the routing functionalities by nodes themselves such as route discovery, topology discovery and delivering messages from source to destination. Clustering provides the finest answer for huge and dense mobile adhoc networks with high mobility. It also lifts the capacity of network and diminishes the routing overhead in order to bring more efficient and effective routing in MANET. There are two mechanisms in every clustering algorithm, (i) cluster formation and (ii) cluster maintenance. In cluster formation, cluster heads are selected among the nodes to form the hierarchical network. Selecting appropriate cluster head is one of the main research issues. In cluster maintenance, a unique mechanism is needed so that the cluster head can maintain the topological information of the cluster in spite of the cluster structure changes every time due to mobility of nodes. This paper mainly focuses on the weight based clustering approaches in MANET.

Keywords – Clustering, Energy, Mobile adhoc network, Mobility.

I. INTRODUCTION

Many WLANs need an infrastructure network. In these infrastructure based wireless networks, communication usually takes place only between the wireless nodes and the access point. The high demand of the long run networks is the speedy deployment of independent mobile nodes that can communicate with each other without the need of a centralized and organized network infrastructure. This type of networks is categorized under the classification of Mobile Ad-hoc Networks (MANETs). A MANET is the collection of mobile devices that comes together to form a network as needed, not necessarily with any support from the existing Internet infrastructure or any other kind of fixed stations. This is in contrast to the well known single-hop cellular network model that supports the needs of wireless communications by installing BSs as access points. In these cellular networks, communication between two mobile nodes relies on the wired backbone and the mounted base stations.

Routing is the most important issue in MANETs. Routing is the process of selecting paths to forward the packets over the network. The primary goal of ad-hoc network routing protocols is to supply correct and economical route establishment between pair of nodes, so the messages are also delivered on time. Route construction should be done with a minimum of overhead and bandwidth consumption. Due to the constraints of power, transmission range and node mobility, path failures are very frequent in this type of networks. To accommodate frequent path failures, special routing protocols are necessary. Basically, routing protocols in MANET can be broadly classified as proactive, reactive, and hybrid routing. In proactive or table-driven protocols, each node maintains a routing table which contains routing information for every reaching node in the network. All the nodes update these tables so as to maintain a consistent and up-to- date view of the network. Some examples of proactive routing protocols are Dynamic Destination Sequenced Distance-Vector (DSDV), Cluster Head and Gateway Switching Routing (CGSR), Wireless Routing Protocol (WRP). These protocols differ in the number of routing related tables and how changes are broadcasted in the network structure. In reactive or on-demand routing, all updated routes are not kept at each node. Routes are generated when needed. When source wants to send data to destination, it invokes a route discovery mechanism to find the path to destination. Some examples of reactive routing protocols are Dynamic Source Routing (DSR), Ad Hoc On-Demand Distance Vector (AODV), Temporally-Ordered Routing Algorithm (TORA). Hybrid protocols combine the benefits of both proactive and reactive routing protocols and overcome their shortcomings. Here, the routing is initially established with some proactively explored routes and then serves the demand from additionally activated nodes through reactive flooding. Zone Routing Protocol (ZRP) is the popular example of hybrid routing protocol.

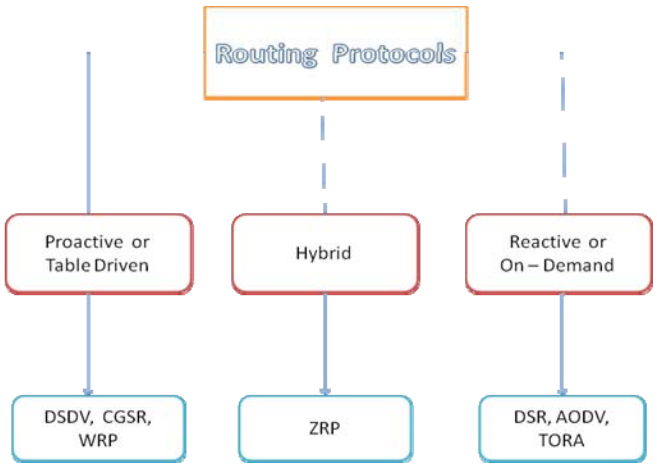

Figure 1. Routing Protocols in MANET

II. CLUSTERING: TYPES & ADVANTAGES

A. Clustering –

Clustering is the virtual partitioning of nodes into sub networks according to geographical area in MANET. A cluster structure makes ad-hoc networks seems to smaller and more stable. Each mobile node in the cluster broadcast the messages to establish connection. If a node changes its cluster then only the nodes which are residing in corresponding clusters are required to update the data, there is no need the changes to be done by the entire network.

The cluster head, cluster members and gateway plays important role in clustering where cluster head and gateway are the backbone nodes in hierarchical ad-hoc network. Cluster-Head (CH) is native organizer of a cluster and Cluster-Member is a standard node. It is a node that is neither a CH nor gateway. Cluster-Gateway is common node between two or more cluster which provides inter cluster links with node to forward information between clusters.

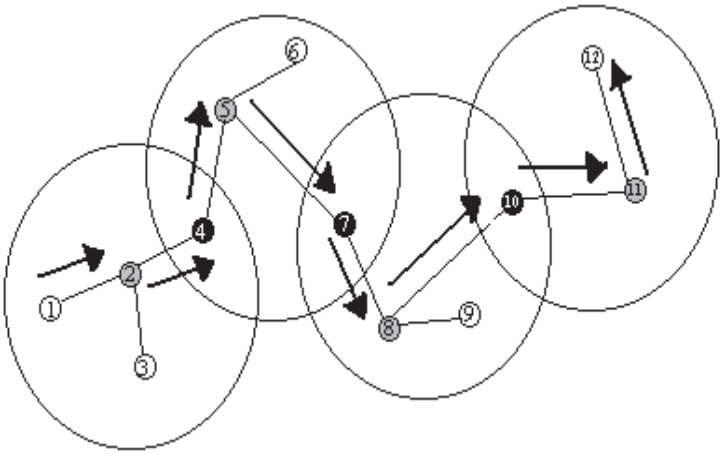

Figure 2. Cluster Structure in MANET

In a cluster, two varieties of communications take place:

Intra-cluster Communication: In this cluster, the cluster head has 1-hop connectivity with each cluster member. Therefore, cluster head will directly communicate with member nodes. However, member nodes cannot directly communicate with other members of cluster.

Inter-cluster Communication: In this cluster communication Multi point relay concept selects the cluster head through which the data packets would be forwarded. This mechanism, minimize the congestion by reducing the number of forwarding nodes and saves the battery power of cluster head.

B. Types of Clustering –

DS-based clustering:- Finding a (weakly) connected dominating set to reduce the number of nodes participating in route search or routing table maintenance. Ex - Connected DS, Weak CDS.

Low-maintenance clustering:- Providing a cluster infrastructure for upper layer applications with minimized clustering-related maintenance cost. Ex- LCC (Least Cluster Change), 3hBAC (3-hop Between Adjacent Clusterheads), PC (Passive Clustering).

Mobility-aware clustering:- Utilizing mobile nodes mobility behavior for cluster construction and maintenance and assigning mobile nodes with low relative speed to the same cluster to tighten the connection in such a cluster. Ex - MOBIC, DDCA (Distributed Dynamic Clustering Algorithm).

Energy-efficient clustering:- Avoiding unnecessary energy consumption or balancing energy consumption for mobile nodes in order to prolong the lifetime of mobile terminals and a network. Ex - IDLBC, Energy based DS.

Load-balancing clustering:- Distributing the workload of a network more evenly into clusters by limiting the number of mobile nodes in each cluster in a defined range. Ex - DLBC (Degree-Load-Balancing Clustering).

Combined-metrics-based clustering:- Considering multiple metrics in cluster configuration, including node degree, mobility, battery energy, cluster size, etc., and adjusting their weighting factors for different application scenarios. Ex- WCA (Weighted Clustering Algorithm),On-Demand WCA.

C. Advantages of Clustering –

Aggregation of Topology Information: Due to the fact that the number of nodes of a cluster is lower than the number of nodes in the whole network. The clustering process assists in aggregating topology information.

Efficiency and Stability: The significant feature of cluster structure is that it causes MANET to seem smaller and more stable. That is, once a mobile node changes its attaching cluster, then the nodes lying within the corresponding clusters unit area needed to alter their routing tables.

Bandwidth Efficiency: Only the cluster heads participates in routing process, and the cluster members deal only with its cluster heads, therefore avoids unneeded exchange of messages among the mobile nodes, thus the use of bandwidth is often improved.

Routing Efficiency: In flat topology, every node bears equal responsibility to act as router for routing the packets to every other node so a great amount of flooding messages takes place in order to obtain better routing efficiency. But, such control packets reduces MAC layer strength. Therefore, cluster structure is often the substitute to boost MAC layer strength and to make the routing process easier.

Spatial Reuse of Resources: In cluster structure, each node is assigned with different role and functionality. That is, each cluster is assigned a leader called cluster head and if a node comes within the transmission range of more than

one cluster will be acting as a gateway node. Hence, by this manner, the cluster topology facilitates resource management.

.

III. WEIGHT BASED CLUSTERING ALGORITHMS

Weighted Clustering Algorithm (WCA) [1]:
This algorithm was originally proposed by M. Chatterjee et al. It considers four parameters for clusterhead selection. They are:

(1) Degree Difference (Δv): It is calculated as $|dv - \delta|$ for every node v. Here, dv denotes degree of a node and δ is a pre-defined threshold.
(2) Distance Summation (Dv): It is defined as the sum of distances from a given node to all its neighbors.
(3) Mobility (Mv): It is taken by computing the running average speed of every node during a specified time T.
(4) Remaining Battery Power (Pv): It is a measure of how much battery power has been consumed.

WCA selects the clusterheads according to the weight value of each node. The weight associated to a node v is defined as: $Wv = w1\ \Delta v + w2\ Dv + w3\ Mv + w4\ Pv$ ---------- (Eq. 1)
The node with the minimum weight is selected as a clusterhead.
The weighting factors are chosen so that $w1 + w2 + w3 + w4 = 1$
The clusterhead selection algorithm finishes once all the nodes become either a clusterhead or a member of a clusterhead.

Adaptive Weighted Cluster Based Routing Protocol (AWCBRP) [2]:
Due to the mobility of nodes Topology changes and breakage of exiting paths occurs repeatedly. A routing protocol should quickly adapt to the topology changes and efficiently search for new paths with minimal power consumption. An adaptive weighted cluster based routing protocol for mobile ad-hoc networks improves speedily to the topological changes and efficiently sets up the routing process.

In this approach, the cluster head selection is performed by assigning a weight value based on the factors Energy Level, Connectivity and Stability.
Cluster heads are selected based on the following weighted sum $W = w1\ D1 + w2\ D2 + w3\ D3$ ---------- (Eq. 2)
Where D1 is the power level of the node, D2 is the connectivity factor and D3 is the stability index and w1, w2 and w3 are the weighting factors. Cluster head has the least W value.

After the determination of cluster head and its cluster member, they will be recognized as “considered". Every unconsidered node goes through the election process. After the selection of “considered nodes” the election algorithm will be finished.

Flexible Weight Based Clustering Algorithm (FWCA) [3]:
FWCA is proposed by Zouhair El-Bazzal et al. It has the flexibility of assigning different weights to the nodes and takes into account a combined metrics to form clusters automatically. Limiting the number of nodes inside a cluster allows restricting the number of nodes provided by a clusterhead so that it does not degrade the MAC functioning.

In this algorithm, firstly the IDs of nodes (node ID) and clusterheads (CH ID) are allocated. These IDs are the MAC addresses. The CH ID appended with the node ID forms a unique identifier for every node. Also, a ‘Counter’ is maintained by each node in order to count the number of nodes inside a cluster and to guarantee that the cluster size does not exceed a predefined ‘N’ in terms of number of nodes by cluster.

Each node Ni (member or CH) is identified by a state such as:
Ni (idnode, idCH, Weight, Counter, N)

It also has to maintain a ‘node_table’ wherein the information of the local members is stored. The CHs maintain another clusterhead information table ‘CH_table’ wherein the information about the other CHs is stored.

Every cluster has a limited number of nodes which defines its size. It also has a CH for communication across the cluster. The nodes collaborate to select the best CH. A CH must be able to manage its members, to accept or to refuse the attachment of new arrivals based on its capacity without concerning the functionality of the other members.

Finally, the weight parameter is periodically calculated by each node in order to indicate the suitability of a node for playing clusterhead's role.

WCA with Mobility Prediction [4]:
A modified version of the Weighted Clustering Algorithm (WCA) is proposed for the cluster formation and mobility prediction for cluster maintenance. The cluster formation is done as in WCA. Mobility Prediction, a quantity is applied to predict whether a node moves along with all its 1-hop neighbors has been done for the cluster maintenance.

Clusterhead (CH) Selection: Election is based on the weight values of the nodes & the node having the lowest weight is chosen as CH.

Cluster Formation: Initially, each node broadcasts a beacon message to notify its presence to the neighbors. A beacon message contains the state of the node. Each node builds its neighbor list based on the beacon messages received.
The cluster-heads Election is based on the weight values of the nodes and the node having the lowest weight is chosen as CH.

Cluster Maintenance: In this phase, the two distinct types of operations are defined as: the battery power threshold property and the node movement to the outside of its cluster boundary.

Entropy-based Weighted clustering algorithm (EWCA) and its Optimization (EWCA-TS) [5]:
Entropy poses uncertainty and is a measure of the disorder in a system. So it is a better indicator of the stability and mobility of the ad hoc network. This algorithm uses an entropy- based model for evaluating the route stability in ad hoc networks and electing clusterhead, thus forming a more stable network than WCA.

The two improvements propose in the EWCA over WCA are:
(1) Replacing only the mobility parameter of equation (A) of WCA by the entropy of local networks in order to reduce the frequency of reaffiliation.

We replace one term of (Eq. 1), the average speed of nodes (Mv), by the entropy defined in (Eq. 3). Hence, the new formula to calculate Wv becomes: $Wv = c1\ \Delta v + c2\ Dv + c3\ (-Hv) + c4\ Pv$ …….. (Eq. 3)
where c1, c2, c3 and c4 are weighing factors.

(2) The Tabu Search Optimized EWCA (EWCA-TS)
Tabu Search is used to optimize the election routine which forms the near optimal dominant set. TS have achieved great success in solving complex combinatorial optimization problems.

Connectivity, Energy & Mobility driven Weighted Clustering Algorithm (CEMCA) [6]:
The idea of CEMCA is to find a number of cluster heads that ensures the stability of the network topology. The election of the cluster head is based on the combination of several significant metrics such as: the lowest node mobility, the highest node degree, the highest battery energy and the best transmission range. This algorithm is completely distributed and all nodes have the same chance to act as a cluster head.

CEMCA is composed of two main stages. The first stage consists in the election of the cluster head and the second stage consists in the grouping of members in a cluster. Normalized value of mobility, degree and energy level is calculated and is used to find the quality (normalized to 1) for each node. The quality of the node is a measure of its

suitability as a cluster head. The node broadcasts its quality to their neighbors in order to compare the better among them. After this, a node that has the best quality is chosen as a clusterhead.

In the second stage the construction of the cluster members set is done. Each clusterhead determines its neighbors at two hops maximum. These nodes form the members of the cluster. Next, each cluster head stores all information about its members and all nodes record the clusterhead identifier. This exchange of information allows the routing protocol to function in the cluster and between the clusters.

Improved Weight Clustering Algorithm (iWCA) [7]:
In this paper, the modification in the weighted clustering algorithm is done such that it can be used in sensor networks with the specific constraints in sensor networks being considered. The addition of one more factor about the characteristic of a sensor node into the evaluation formula is considered, such that the nodes chosen as cluster heads may have a better behavior in heterogeneous sensor networks than those without the additional factor.
Calculate the combined weight for every node v: $Wv = w1\Delta v + w2\,Dv + w3\,Mv + w4\,Tv + w5\,Cv$……(Eq. 4)
Choose the node with a minimum Wv as the cluster head

The cluster heads chosen will act as the application nodes in a two-tired wireless sensor network and may change in different time intervals. After a fixed interval of time, this algorithm is re-run again to add new applications nodes such that the system lifetime can be expected to last longer.

Distributed Weighted Clustering Algorithm (DWCA) [8]:
This approach is based on combined weight metric that takes into account several system parameters like the ideal node degree, transmission range, energy and mobility of the nodes. Depending on specific applications some of these parameters can be used in the metric to determine the clusterhead. However more clusterheads lead to extra number of hops for a packet when it is to be routed from source to destination.

The goals of the algorithm are maintaining stable clustering structure, minimizing the overhead for the clustering set up and maintenance, maximizing lifespan of mobile nodes in the system and achieving good end-to-end performance. DWCA chooses locally optimal clusterheads and incorporates power management at the clusterheads.

Distributed Score Based Clustering Algorithm (DSBCA) [9]:
This algorithm considers the Battery Remaining, Number of Neighbors, Number of Members, and Stability in order to calculate the node's score with a linear algorithm. After each node calculates its score independently, the neighbors of the node must be notified about it. Also each node selects one of its neighbors with the highest score to be its cluster head and, therefore the selection of cluster heads is performed in a distributed manner with most recent information about current status of neighbor nodes.

Each node calculates its score by using a formula that considers all the above parameters. The score of node N is defined as Eq. 5. Score= ((Br×C1) + (Nn×C2) +(S×C3) + (Nm×C4)) …….. (Eq. 5)
Where C1, C2, C3, C4 are the score factors for the corresponding system parameters listed below:

Battery Remaining (Br): The residual node's energy. The energy is consumed through transmitting / receiving data packets and messages.
Number of Neighbors (Nn): The number of existing nodes which are located in the transmission range.
Stability(S): The total time in which the neighbors of a specific node have spent their time beside the node. A Higher stability simply means that the neighbors of a certain node has spent a longer time in its transmission range.
Number of Members (Nm): Set of nodes that is handled by each cluster head.

DSBCA was compared through simulation with WCA and DWCA in terms of number of clusters, number of re-affiliations, lifespan of nodes in the system, end-to-end throughput, overhead and gives better results.

Improved Distributed Weighted Clustering Algorithm (DWCAIMP) [10]:
This approach is based on combined weight metric that takes into account several system parameters like the node degree, transmission range, energy and mobility of the nodes. This algorithm can be divided into three phases - Clusters Formation, Running Mobility and Cluster Maintenance.

Cluster Formation: Initially each node is assigned a random ID value. It broadcasts its ID value to its neighbours and builds its neighbourhood table. Each node calculates its own weight based on the following factors:

- *Node connectivity*: The number of nodes that can communicate directly with the given node i.e. that are in its transmission range.
- *Battery Power*: The power currently left in each node. The energy is consumed by sending and receiving of messages.
- *Mobility*: Running average of speed of each node. If mobility is less, the node is more suitable to become clusterhead.
- *Distance*: Sum of distance of the node from all its neighbours.

$$W = w_1 * c + w_2 * e + w_3 * M + w_4 * d \quad \text{..... (Eq. 6)}$$

Each node calculates its weight by (Eq. 6). Then each node broadcasts its weight to its neighbours. If it has maximum weight among its neighbours, it sets the clhead variable to 1, otherwise, the clhead variable is set to 0. Otherwise, the clhead variable is set to 0. The node with maximum weight broadcasts clhead message to other nodes.

Mobility: A random value is assigned between 0 and 1 to each node and a threshold value is taken. If this random value is greater than threshold value, the node becomes mobile and its *x* and *y* parameters changes, otherwise it remains stationary. A node on reaching new destination joins the nearest clusterhead.

Cluster Maintenance: Cluster maintenance is needed in two cases:

(1) When a node is added in the cluster, then even if the weight is more than the clusterhead it does not immediately become the clusterhead and thus reduces the unnecessary overhead in selection of the clusterhead each time a new node is added.
(2) When a clusterhead fails, then the nodes attached to that clusterhead recalculate their weights and select new clusterhead with the maximum weight.

IV.CONCLUSION

In this paper the survey of various weight based clustering schemes have been done. The methods adopted in finding the clusterhead are different in these algorithms. This paper presents a survey of clustering algorithms in which multiple metrics have been used to find clusterhead based on the weight values of the node with other important matrices or parameters are taken into consideration. I hope that the survey presented in this paper will be helpful and provide researchers a platform for choosing the right weight based clustering algorithm for their work in future.

REFERENCES

[1] M. Chatterjee, S. Das and D. Turgut, "WCA: A weighted clustering algorithm for mobile ad hoc networks", *Cluster computing Journal*, Vol. 5, No. 2, pp. 193–204, 2002.

[2] S. Karunakaran and P. Thangaraj, "An adaptive weighted cluster based routing (AWCBRP) protocol for mobile ad-hoc networks", *WSEAS Transactions on communications*, Vol. 7 , No. 4, pp. 248-257, 2008.

[3] Z. El.Bazzal, M. Kadoch, B. L. Agba, F. Gagnon and M. Bennani, "A flexible weight based clustering algorithm in mobile ad hoc networks", *International Conference on Systems and Networks Communications*, pp. 50, Tahiti, 2006.

[4] S.Muthuramalingam, R.RajaRam, Kothai Pethaperumal and V.Karthiga Devi, "A Dynamic Clustering Algorithm for MANETs by modifying Weighted Clustering Algorithm with Mobility Prediction", *International Journal of Computer and Electrical Engineering*, Vol. 2, No. 4, pp. 709-714, 2010.

[5] Y.X. Wang and F. S. Bao, "An Entropy-based Weighted Clustering Algorithm and Its Optimization for Ad hoc Networks", *published on 3rd IEEE Int'l Conf. on Wireless and Mobile Computing, Networking and Communications, (WiMOB 2007),* 2007.

[6] F.D.Tolba, D. Magoni and P. Lorenz, "Connectivity, energy & mobility driven Weighted clustering algorithm", *in proceedings of IEEE GLOBECOM (2007),* 2007.

[7] U.Maheswari and G. Radhamani, "Clustering Schemes for Mobile Adhoc Networks : A Review", *International Conference on Computer Communication and Informatics (ICCCI -2012),* January 10 – 12, Coimbatore, INDIA, 2012.

[8] W. Choi and M. Woo, "A Distributed Weighted Clustering Algorithm for Mobile Ad Hoc Networks", *Proceedings of Advanced International Conference on Telecommunications and International Conference on Internet and Web Applications and Services,* 2006.

[9] S. Adabi, S. Jabbehdari, A. Rahmani and S. Adabi, "A Novel Distributed Clustering Algorithm for Mobile Adhoc Networks", *Journal of Computer Science,* Vol. 4, No. 2, pp. 161-166, 2008.

[10] N. Chauhan, L. K. Awasthi, N.Chand, V. Katiyar and A. Chugh,"A distributed weighted cluster based routing protocol for MANETs", *Wireless Sensor Network,* Vol. 3, No. 2, pp. 54 – 60, 2011.

Hybrid Algorithm Implemented on Color Image to Design Watermark Image with PSNR & MSE baesd on Cryptography

Garima Sharma
Department of Computer Science and Engineering
KIIT College of Engineering, Gurgaon, Haryana –122102

Shweta Tyagi
Department of Computer Science and Engineering
KIIT College of Engineering, Gurgaon, Haryana –122102

Sharvan Rewri
Assistant Professor
KIIT College of Engineering, Gurgaon, Haryana -122102

Abstract- Visual Cryptography (VC) is a method of encrypting a secret image into shares such that stacking a sufficient number of shares reveals the secret image. During the past decade, with the development of information digitalization and internet, digital media increasingly predominate over traditional analog media. Watermarking is the technique of embedding a secret image into a cover image without affecting its perceptual quality so that secret image can be revealed by some process. Share generation for the visual cryptography can also be done using watermarking technique. We can use these watermarked shares for retrieving the hidden information. This effort can generate the meaningful shares rather than some shares having no information.

Keywords – cryptography, encryption, digital watermarking, host image, spatial domain, predictive coding, patch work, wavelet and discrete cosine transform.

I. INTRODUCTION

Visual cryptography is a cryptographic technique which allows visual information (pictures, text, etc.) to be encrypted in such a way that decryption becomes a mechanical operation that does not require a computer. Such a technique thus would be lucrative for defense and security. Unlike conventional cryptographic methods, VC needs no complicated computation for recovering the secret image. The act of decryption is to simply stack shares and view the secret image that appears on the stacked shares. Visual cryptographic technique is being used by several countries for secretly transfer of images in army, hand written documents, financial documents, text images, internet- voting etc. The digital watermark is then introduced to solve this problem. Covering many subjects such as signal processing, communication theory and Encryption, the research in digital watermark is to provide copyright protection to digital products, and to prevent and track illegal copying and transmission of them. Watermarking is embedding information, which is able to show the ownership or track copyright intrusion, into the digital image, video or audio. Its purpose determines that the watermark should be indivisible and robust to common processing and attack. The proposed scheme adds the advantages of both visual cryptography as well as invisible watermarking technique. Visual cryptography encryption adds the advantage and security of basic scheme. Watermarking is used for embedding shares into cover image without affecting its perceptual quality so that the secret image's share can be revealed by watermark extraction process.

II. BACKGROUND

With the rapid advancement of network topology, multimedia information is transmitted over the Internet conveniently. Various confidential data such as military maps and commercial identification are transmitted over the Internet. While using secret images, security issues should be taken into consideration because hackers may utilize weak link over communication network to steal information that they want. To deal with security problems of secret images, we should develop some secure appropriate algorithm by which we can secure our data on internet. . Practically, this can be done by printing each share on a separate transparency and then placing all of the transparencies on top of each other. In their technique n-1 shares reveals no information about the original image. We can achieve this by using one of following access structure schemes
Figure shows two of the several approaches for (2, 2) – Threshold VCS. In this particular figure first approach shows that each pixel is broken into two sub pixels. Let B shows black pixel and T shows Transparent (White) pixel. Each share will be taken into different transparencies. When we place both transparencies on top of each other we get following combinations, for black pixel BT+TB=BB or TB+BT=BB and for white pixel BT+BT=BT or TB+TB=TB. Similarly second approach is given where each pixel is broken into four sub pixels. We can achieve 4C2 =6 different cases for this approach

1: Each Pixel is broken into two sub pixels as follows.

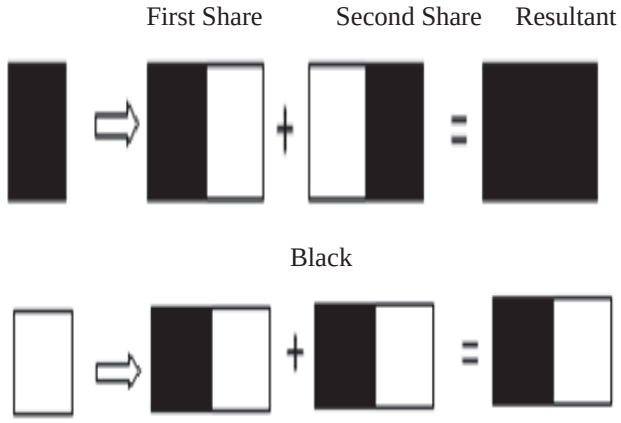

2: Each Pixel is broken into four sub pixels as follows.

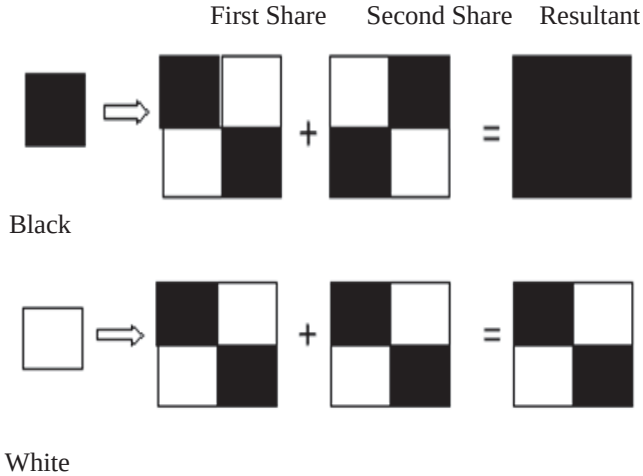

Fig. 1 Pixel is broken into four sub pixel

III. DESCRIPTION OF SYSTEM DESIGN AND METHODOLOGY

Information hiding can be mainly divided into three processes - cryptography, stenography and watermarks. Cryptography is the process of converting information to an unintelligible form so that only the authorized person with the key can decipher it. Stenography is the process of hiding information over a cover object such that the hidden information cannot be perceived by the user. Watermarking is closely related to stenography, but in watermarking the hidden information is usually related to the cover object. Hence it is mainly used for copyright protection and owner authentication.

Principle of Watermarking:

A watermarking system is usually divided into three distinct steps, embedding, attack and detection. In embedding, an algorithm accepts the host and the data to be embedded and produces a watermarked signal. The watermarked signal is then transmitted or stored, usually transmitted to another person. If this person makes a modification, this is called an attack. There are many possible attacks. Detection is an algorithm which is applied to the attacked signal to attempt to extract the watermark from it [1-2]. If the signal was not modified during transmission, then the watermark is still present and it can be extracted. If the signal is copied, then the information is also carried in the copy. The embedding takes place by manipulating the content of the digital data, which means the information is not embedded in the frame around the data, it is carried with the signal itself. Figure 2 shows the basic block diagram of watermarking process.

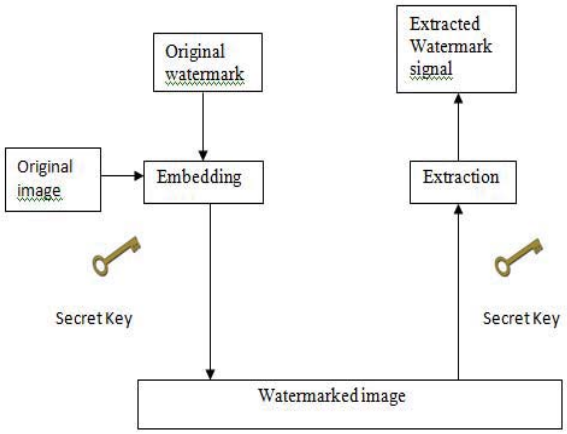

Fig. 2 Watermarking block diagram

*Classification of Watermarking***:**

It can be classified in visible and invisible watermarking.

- Visible:The watermark is visible which can be a text or a logo used to identify the owner.

Any text or logo to verify or hide content

$Fw= (1-\alpha)\ F+ \alpha*W$

Fw = Watermarked Image

α =constant; $0<=\alpha<=1$, IF $\alpha=0$ No watermark, if $\alpha=1$ watermark present

F =original image

W =watermark

- Invisible:The watermark is embedded into the image in such a way that it cannot be perceived by human eye. It is used to protect the image authentication and prevent it from being copied. Invisible watermark can be further divided into three types. Robust Watermarks, Fragile Watermarks, Public and Private Watermark

A. *Techniques of Watermarking*

Digital watermarking is addressed mostly in spatial or frequency domain. Based on application's requirement different watermarking techniques can be selected. Most of the present work in the area of digital watermarking is inspired by the manipulating the frequency domain of the multimedia objects. In frequency domain, researchers have selected different transformation methods for embedding and extracting watermark objects. These includes Discrete Cosine Trans-form (DCT), Discrete Fourier Transform (DFT) and Wavelets.

1) *Frequency Domain techniques:* Frequency domain watermarking technique is also called transform domain. Values of certain frequencies are altered from their original. Typically, these frequency alterations are done in the lower frequency levels, since alterations at the higher frequencies are lost during compression. Watermarking in the frequency domain involves embedding in the image's transform coefficients.

2) *Discrete Cosine Transform (DCT) Technique:* Discrete cosine transform (DCT): It is a process which converts a sequence of data points in the spatial domain to a sum of sine and cosine waveforms with different amplitudes in the frequency domain. The DCT is a linear transform, which maps an n-dimensional vector to set of n coefficients [3-5]. A linear combination of n known basis vectors weighted with the n coefficients will result in the original vector. The known basis vectors of transforms from this class are "sinusoidal", which means that they can be represented by sinus shaped waves or, in other words, they are strongly localized in the frequency spectrum. Therefore one speaks about transformation to the frequency domain. The most popular member of this class is the Discrete Fourier Transformation (DFT).The difference between DCT and DFT is that DFT applies to complex numbers, while DCT uses just real numbers. For real input data with even symmetry DCT and DFT are equivalent.

The coefficients can be split using the zigzag ordering into low frequency coefficients, mid frequency coefficients and high frequency coefficients as shown in Fig.3

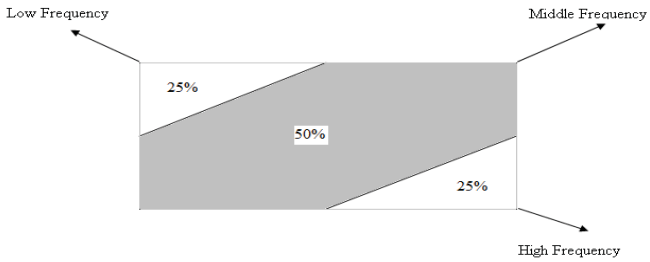

Fig. 3 DCT Decomposition

Figure 4 shows the structure of the proposed scheme. The proposed scheme generates the VC shares using basic visual cryptography model and then embed them into a cover image using invisible blind watermarking technique, so that the secret shares[6-7] will be more secure, meaningful and shares are protected from the malicious adversaries who may alter the bit sequences to create the fake shares. During the decryption phase, secret shares are extracted from the respective cover images without using any cover image characteristics to provide mutual authentication

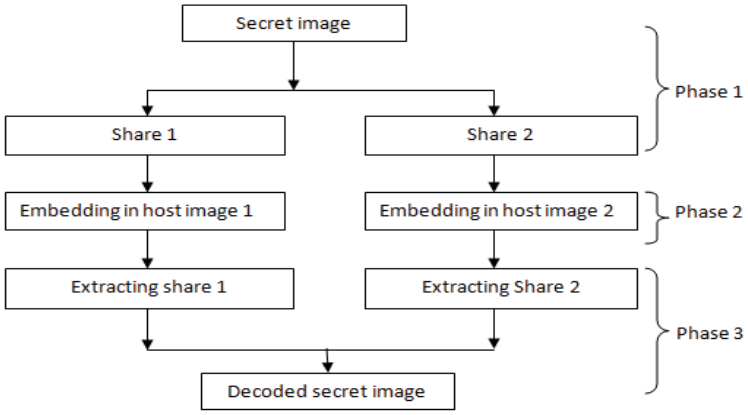

Fig. 4 Structure of the Proposed Scheme

Any single share is a random choice of two black and two white sub pixels, which looks medium grey. Fig.5 shows share creation using VC (2, 2) Encryption. When two shares are stacked together, the result is either medium grey (which represents white) or completely black (which represents black).

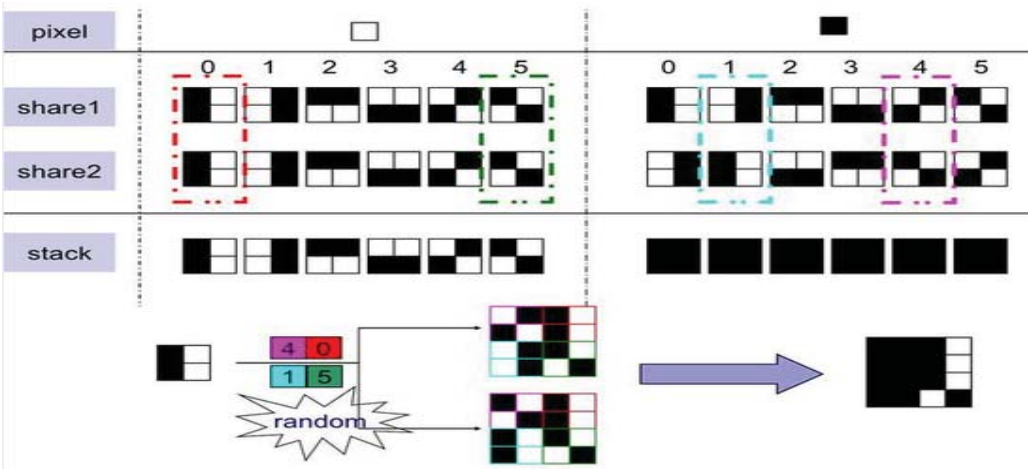

Fig. 5 Share creation using VC (2, 2) encryption Scheme

IV. RESULT

RESULT I: Peak Signal to Noise Ratio

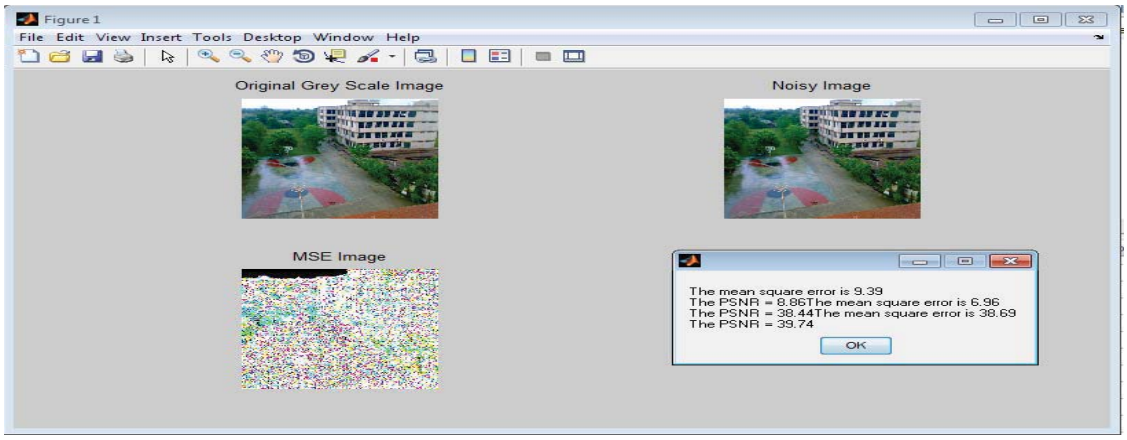

Fig. 6 show PSNR and RMSE of different images

TABLE I

PSNR & MSE of Different Image

Sr. No.	Types of Images	PSNR	MSE
1	Original Gray scale image	8.86	9.39
2	Noisy Image	38.44	6.96
3	Mean Square Error image	39.74	38.69

RESULT II: Sharpe Images

In result II we calculated the sharp images elapsed time from given watermark images. As shown in figure 7 which are watermark images and then determine extracted secret message then shared and finally revealed message.

(a)

(b)

(c)

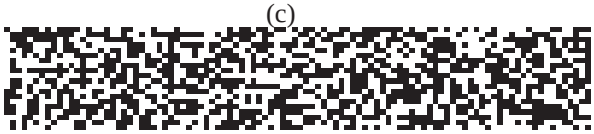

(d)

(e)

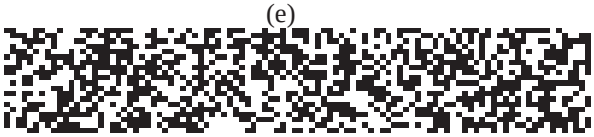

(f)

Fig. 7 show watermark images (a, b) and then determine extracted secret message(c, d) then shared and finally revealed message (e, f)

- Elapsed time of first image is=1.3260
- Elapsed time of first image is=0.9828

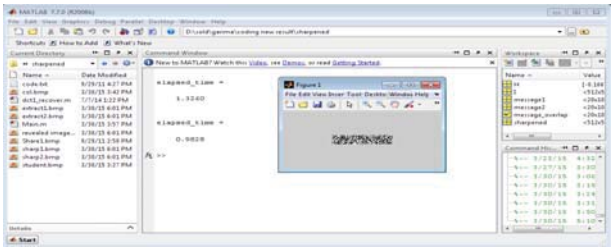

Fig.8 Elapsed time of Fig.7 images

In the same way we calculate result for blurred image and extracted secret image, shared image and finally revealed image of both image and their processing time.

- Elapsed time of first image is=1.2324
- Elapsed time of first image is=0.9828

RESULT IV: Blurred Images

Fig.9 original image of size 40*15

Fig.10 extract1 message of Fig.9

Fig.11 extract2 message of Fig.9

Fig.12 share1 message of Fig.9

Fig.13 share1 message of Fig.9

Fig.14 output message of Fig.9

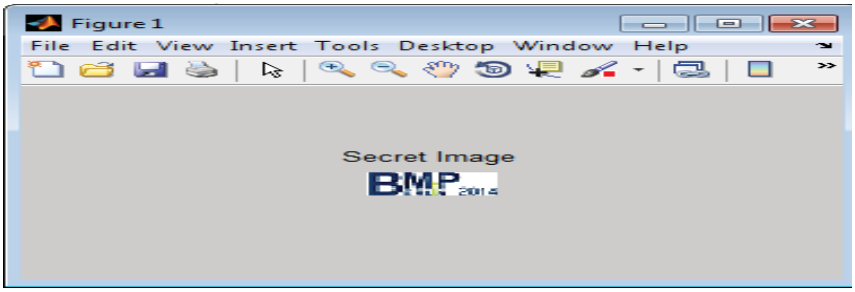

Fig.15 secret message

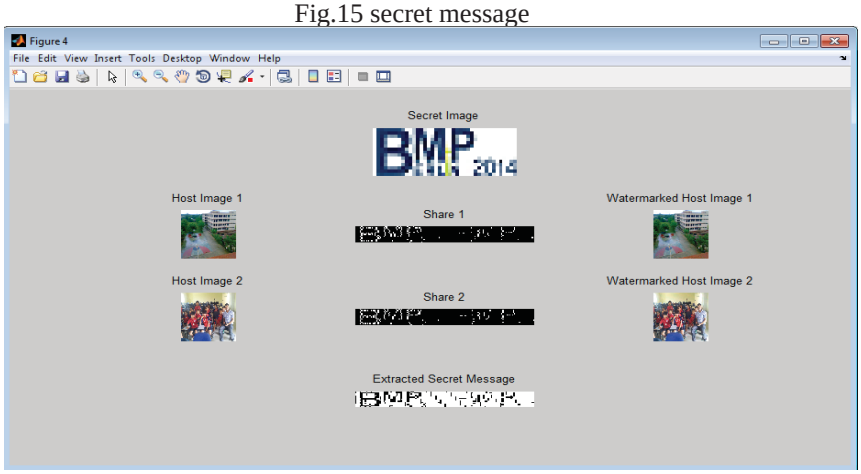

Fig.16 show Snapshot of all images obtained by cryptography ie host image1, 2 and watermark image1, 2, secret message, share1, share2, extracted secret message

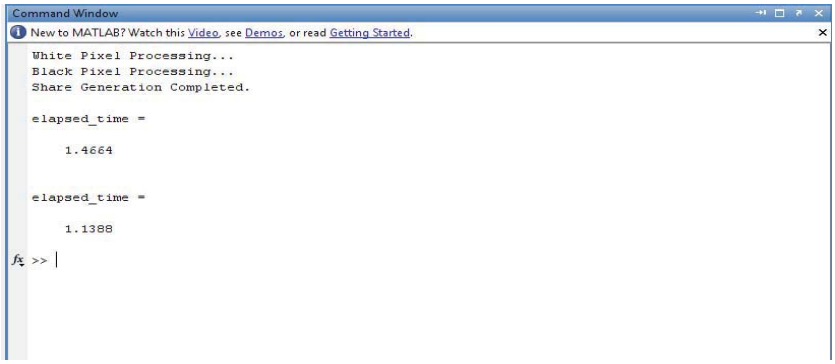

Fig. 17 white and black pixel processing time of image is listed below
White and Black pixel processing time:

- White pixel processing Time:1.4664
- Black Pixel processing time:1.1388

V. CONCLUSION

The proposed scheme used visual cryptography for share generation and each share is embedded in a cover image using digital watermarking. Visual cryptography encryption adds the advantage and security of basic scheme. Watermarking provided double security to shares by hiding them in some cover images. Watermarked images are robust against a number of attacks like blurring, sharpening, cropping etc.

REFERENCES

[1] B.padhmavati, P.Nirmal Kumar, M.A.Dorai Rangaswamy, 2010. A Novel Scheme for Mutual Authentication and Cheating Prevention in Visual Cryptography Using Image Processing. In *Proceedings of International Conference on Advances in Computer Science 2010* DOI: 02, ACS.2010.01.264, ACEEE.

[2] E. R. Verheul and H. C. A. Van Tilborg, "Constructions and properties of out of visual secret sharing schemes," *Designs, Codes, Cryp- tography*, vol. 11, no. 2, pp. 179-196, May 1997.

[3] H. Hajiabolhassan and A. Cheraghi, "Bounds for visual cryptography schemes," *Discrete Appl. Math.*, vol. 158, no. 6, pp. 659-665, Mar. 2010.

[4] D.Jena and S.Jena, 2009. A Novel Visual Cryptography Scheme. In Proceedings of International Conference on Advanced Computer Control, (ICACC'2009), pp.207-211.

[5] Mrs.D.Mathivadhani, Dr.C.Meena, 2010. Digital Watermarking and Information Hiding using Wavelets, SLSB and Visual Cryptography method. In *Proceedings of International Conference on Computational Intelligence and Computing Research (ICCIC'2010)*, pp. 1-4.

[6] S. J. Shyu, "Image encryption by random grids," *Pattern Recognit.*, vol. 40, no. 3, pp. 1014-1031, Mar. 2007.

[7] M.Naor and A.Shamir, 1995. Visual cryptography. *Advances in Cryptology EUROCRYPT '94*. Lecture Notes in Computer Science, (950):1–12.

[8] P.S.Revenkar, Anisa Anjum, W.Z.Gandhare, 2010. Survey of Visual Cryptographic Schemes. *International Journal of Security and Its Applications*, Vol. 4, No. 2, April, 2010.

[9] S.Punitha, S.Thompson, N.Lingam, 2010. Binary Watermarking Technique based on Visual Cryptography. In *Proceedings of International Conference on Communication Control and Computing Technologies (ICCCCT'2010)*, pp. 232-235.

[10] S.Riaz, M.Javed and M.Anjum, 2008. Invisible Watermarking Schemes in Spatial and Frequency Domains. In *Proceedings of fourth International Conference on Emerging Technologies (ICET' 2008)*, pp. 211-216.

[11] Y.Bani, Dr.B.Majhi and R.S.Mangrulkar, 2008. A Novel Approach for Visual Cryptography Using a Watermarking Technique. In *Proceedings of 2nd National Conference, IndiaCom 2008*.

[12] F. Liu, C. K. Wu, and X. J. Lin, "A new definition of the contrast of visual cryptography scheme," *Inf. Process. Lett.*, vol. 110, no. 7, pp. 241-246, Mar. 2010.

[13] R. Z. Wang, "Region incrementing visual cryptography," *IEEE Signal Process. Lett.*, vol. 16, no. 8, pp. 659-662, Aug. 2009.

[14] P. A. Eisen and D. R. Stinson, "Threshold visual cryptography schemes with specified whiteness levels of reconstructed pixels," *Designs, Codes, Cryptography*, vol. 25, no. 1, pp. 15-61, 2002.

[15] Y.Bani, Dr.B.Majhi and R.S.Mangrulkar, 2008. A Novel Approach for Visual Cryptography Using a Watermarking Technique. In *Proceedings of 2nd National Conference, IndiaCom 2008*.

[16] G. B. Horng, T. G. Chen, and D. S. Tsai, "Cheating in visual cryptography," *Designs, Codes, Cryptography*, vol. 38, no. 2, pp. 219-236, Feb. 2006.

[17] R. Ito, H. Kuwakado, and H. Tanaka, "Image size invariant visual cryptography," IEICE Trans. Fundam. Electron., Commun., Comput. Sci., vol. 82, pp. 2172-2177, Oct. 1999.

[18] S.Riaz, M.Javed and M.Anjum, 2008. Invisible Watermarking Schemes in Spatial and Frequency Domains. In *Proceedings of fourth International Conference on Emerging Technologies (ICET' 2008)*, pp. 211-216.

[19] R. Ito, H. Kuwakado, and H. Tanaka, "Image size invariant visual cryptography," IEICE Trans. Fundam. Electron., Commun., Comput. Sci., vol. 82, pp. 2172-2177, Oct. 1999.

[20] F. Liu, C. K. Wu, and X. J. Lin, "Colour visual cryptography schemes," *IET Inf. Security*, vol. 2, no. 4, pp. 151-165, Dec. 2008.

[21] G. Ateniese, C. Blundo, A. De Santis, and D. R. Stinson, "Visual cryptography for general access structures," *Inf. Computat.*, vol. 129, no. 2, pp. 86-106, Sep. 1996.

An Advance Approach to Compress Binary and Color image using Discrete Cosine Transform (DCT) and Analysis of Gamma Factor on Images

Shweta Tyagi
Department of Computer Science and Engineering
KIIT College of Engineering, Gurgaon, Haryana –122102

Garima Sharma
Department of Computer Science and Engineering
KIIT College of Engineering, Gurgaon, Haryana –122102

Sharvan Rewri
Assistant Professor
KIIT College of Engineering, Gurgaon, Haryana -122102

Abstract- Image compression is one of the basic problems in the field of image transmission through internet and to store in digital form on computers. There are lot of technique for compressing an image and we have to compress in such a way that all the precious data must be preserved with good quality that why it become very tedious task to compress an image. We implemented hybrid algorithm using Huffman coding to achieve the desire result. Our main aim is to get peak signal to noise ratio, mean square error, compression ratio and CPU processing time for DCT and IDCT. This work can be extended for the detection of Double JPEG compression. DOUBLE Joint Photographic experts group (JPEG) compression means that a JPEG image will be compressed once again by JPEG compression. The detection of double JPEG compression is of great significance in digital forensics.

Keywords – Compression, DCT, MSE, peak signal to noise ratio, scaling factor, spatial domain

I. INTRODUCTION

Image compression, the art and science of reducing the amount of data required to represent an image, is one of the most useful and commercially successful technology in the field of digital image processing. The number of images that are compressed and decompressed daily is staggering. Web page images and high resolution digital camera photos also are compressed routinely to save storage space and reduce transmission time. Compression of digital images with the help of discrete cosine transform (DCT).Several encoding technique have also been used together with DCT to improve the performance of compression. Image may be defined as a two-dimensional function, f(x, y), where x and y are spatial (plane) coordinates, and the amplitude of f(x, y) at any pair of coordinates (x, y) is called the intensity or gray level of the image at that point. When x, y and the amplitude values of f are all finite, discrete quantities, we call the image a digital image. Images as Matrices:
The coordinate system leads to the following representation of a digitized image function:

$$f(x, y) = \begin{matrix} f(0,0) & f(0,1) \ldots\ldots\ldots\ldots\ldots & f(0,N-1) \\ f(1,0) & f(1,1) \ldots\ldots\ldots\ldots\ldots & f(1,N-1) \\ f(M-1,0) & f(M-1,1) \ldots\ldots\ldots\ldots & f(M-1,N-1) \end{matrix}$$

Each element of this array is called an image element, pixel, picture element or pel. A 1*N matrix is called a row vector and M*1 matrix is called a column vector. A 1*1 matrix is called a scalar.

II. BACKGROUND

Image compression is very important for efficient transmission and storage of images. Demand for communication of multimedia data through the telecommunications network and accessing the multimedia data through Internet is growing explosively. With the use of digital cameras, requirements for storage, manipulation, and transfer of digital images has grown explosively. A gray scale image that is 256 x 256 pixels has 65, 536 elements to store, and a typical 640 × 480 color image has nearly a million. Image compression standards bring about many benefits, such as:

(1) Easier exchange of image files between different devices and applications in small time.
(2) Reuse of existing hardware and software for a wider array of products.
(3) Existence of benchmarks and reference data sets for new and alternative developments.
(4) Bandwidth requirement for image transmission also decreases considerably with the increase in compression.

III. DESCRIPTION OF SYSTEM DESIGN AND METHODOLOGY

Predictive coding such as Delta Predictive Code Modulation and Adaptive Delta Predictive Code Modulation were popular for image compression. . In predictive coding, information already sent or available is used to predict future values, and the difference is coded. Transform coding, on the other hand, first transforms the image from its spatial domain representation to a different type of representation using some well known transform and then codes the transformed values (coefficients). This method provides greater data compression compared to predictive methods. DCT algorithms are capable of achieving a high degree of compression with only minimal loss of data. After the DCT coefficient reduction lossless encoding results a higher compression ratio in JPEG as it was not possible with Predictive coding. DCT based image compression technique with Huffman.

As shown on fig 1 Firstly we divide the image into blocks. At this step we also specify the size of block. Then each block of image are subjected to discrete cosine transform. After that each transformed block of image is divided by standard JPEG table, we can set the coefficient of quantization table by scaling factor. At Final step we applied Huffman Encoding over the quantized coefficient. After processing of all blocks algorithm will stop.

Spatial domain versus Transform domain compression: Predictive coding is a spatial domain technique. In predictive coding, information already sent or available is used to predict future values, and the difference is coded. Transform coding, on the other hand, first transforms the image from its spatial domain representation to a different type of representation using some well-known transform and then codes the transformed values (coefficients).

Image Compression Model: First we apply original image then following procedure carried out and finally got compressed image and decoder is its inverse procedure only. In decoder we apply compressed image then inverse transform followed by de quantization and finally lossless entropy decoding.

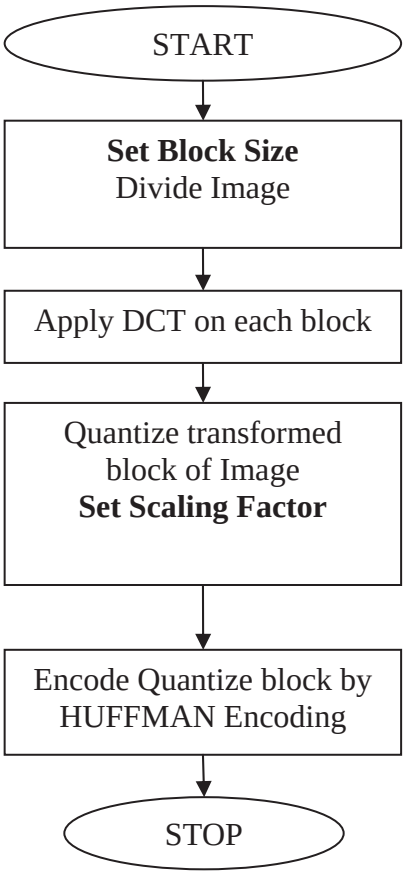

Fig.1 Flow Chart for DCT Image compression with Huffman Encoding

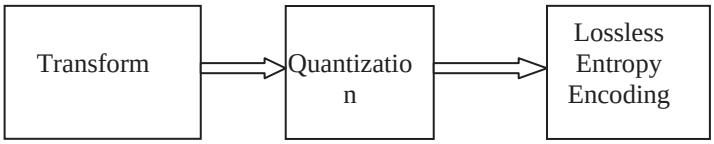

Fig.2 Encoder for Image compression

Discrete Cosine Transform: Discrete Cosine Transform (DCT) is a Fourier-related transform similar to the Discrete Fourier Transform (DFT), but using only real numbers. It transforms a signal or image from the spatial domain to the frequency domain DCT is a mechanism used in the JPEG compression algorithm to transform successive 8×8-pixel blocks of the image from spatial domain to 64 DCT coefficients in each frequency domain. The discrete cosine transform of a list of n real numbers p(x, y), is given by

$$D(i,j) = \frac{1}{\sqrt{2N}} C(i)C(j) \sum_{x=0}^{N-1} \sum_{y=0}^{N-1} P(x,y) \cos\left[\frac{(2x+1)i\pi}{2N}\right] \cos\left[\frac{(2y+1)j\pi}{2N}\right] \quad (3.1)$$

$$c(u) = \begin{cases} \frac{1}{\sqrt{2}} & \text{if } u = 0 \\ 1 & \text{if } u > 0 \end{cases}$$

$$D(i,j) = \frac{1}{\sqrt{2N}} C(i)C(j) \sum_{x=0}^{7} \sum_{y=0}^{7} P(x,y) \cos\left[\frac{(2x+1)i\pi}{2N}\right] \cos\left[\frac{(2y+1)j\pi}{2N}\right] \quad (3.3)$$

P (x,y) is the x, y^{th} element of the image represented by the matrix P. N is the size of the block. The equation calculates one entry (i,jth) of the transformed image from the pixel values of the original image matrix.
Consider the example of 8*8 sub image.

$$\begin{pmatrix} 52 & 55 & 61 & 66 & 70 & 61 & 64 & 73 \\ 63 & 59 & 55 & 90 & 109 & 85 & 69 & 72 \\ 62 & 59 & 68 & 113 & 144 & 104 & 66 & 73 \\ 63 & 58 & 71 & 122 & 154 & 106 & 70 & 69 \\ 67 & 61 & 68 & 104 & 126 & 88 & 68 & 70 \\ 79 & 65 & 60 & 70 & 77 & 68 & 58 & 75 \\ 85 & 71 & 64 & 59 & 55 & 61 & 65 & 83 \\ 87 & 79 & 69 & 68 & 65 & 76 & 78 & 94 \end{pmatrix}$$

After the subtraction of 128 from greay levels is presented below:

$$\begin{pmatrix} -76 & -73 & -67 & -62 & -58 & -67 & -64 & -55 \\ -65 & -69 & -73 & -38 & -19 & -43 & -59 & -56 \\ -66 & -69 & -60 & -15 & 16 & -24 & -62 & -55 \\ -65 & -70 & -57 & -6 & -26 & -22 & -58 & -59 \\ -61 & -67 & -60 & -24 & -2 & -40 & -60 & -58 \\ -49 & -63 & -68 & -58 & -51 & -60 & -70 & -53 \\ -43 & -57 & -64 & -69 & -73 & -67 & -63 & -45 \\ -41 & -49 & -59 & -60 & -63 & -52 & -50 & 34 \end{pmatrix}$$

The next step is to take the two-dimensional DCT, which is given by:

$$\begin{pmatrix} -415 & -30 & -61 & 27 & 56 & -20 & -2 & 0 \\ 4 & -22 & -61 & 10 & 13 & -7 & -9 & 5 \\ -47 & 7 & 77 & -25 & -29 & 10 & 5 & -6 \\ -49 & 12 & 34 & -15 & -10 & 6 & 2 & 2 \\ 12 & -7 & -13 & -4 & -2 & 2 & -3 & 3 \\ -8 & 3 & 2 & -6 & -2 & 1 & 4 & 2 \\ -1 & 0 & 0 & -2 & -1 & -3 & 4 & 1 \\ 0 & 0 & -1 & -4 & -1 & 0 & 1 & 2 \end{pmatrix}$$

The large value of the top-left corner represent DC coefficient. The remaining 63 coefficients are called the AC coefficients. The advantage of the DCT is its tendency to aggregate most of the signal in one corner of the result, as may be seen above.

PSNR (Peak Signal to Noise Ratio)

$$PSNR = 10\log_{10} \frac{255^2}{MSE}$$

Mean Square Error (MSE)

$$MSE = (1/M \times N)\sum_{i=1}^{M}\sum_{j=1}^{N}(a_{ij} - b_{ij})^2$$

Where MSE is the mean squared difference between the compressed and original images.

Compression Ratio: If n1 and n2 denote the number of information carrying units in original and compressed image respectively, then the compression ratio CR can be defined as

CR=(n1/n2);

IV. RESULT

We have presented the relationship between the compression ratio and the scaling factor of quantization tables. The default quantization table which is mostly employed for DCT based image compression is defined as

$$t = \begin{pmatrix} 16 & 11 & 10 & 16 & 24 & 40 & 51 & 61 \\ 12 & 12 & 14 & 19 & 26 & 58 & 60 & 55 \\ 14 & 13 & 16 & 24 & 40 & 57 & 69 & 56 \\ 14 & 17 & 22 & 29 & 51 & 87 & 80 & 62 \\ 18 & 22 & 37 & 56 & 68 & 109 & 103 & 77 \\ 24 & 35 & 55 & 64 & 81 & 104 & 113 & 92 \\ 49 & 64 & 78 & 87 & 103 & 121 & 120 & 101 \\ 72 & 92 & 95 & 98 & 112 & 100 & 103 & 99 \end{pmatrix}$$

Now we are listing our result in which according to quality we receive different DCT CPU processing time compression ratio, inverse DCT CPU time and peak signal to noise ratio. And after that gamma correction result of different images are list and after that region growing result of JPEG image will be listed.

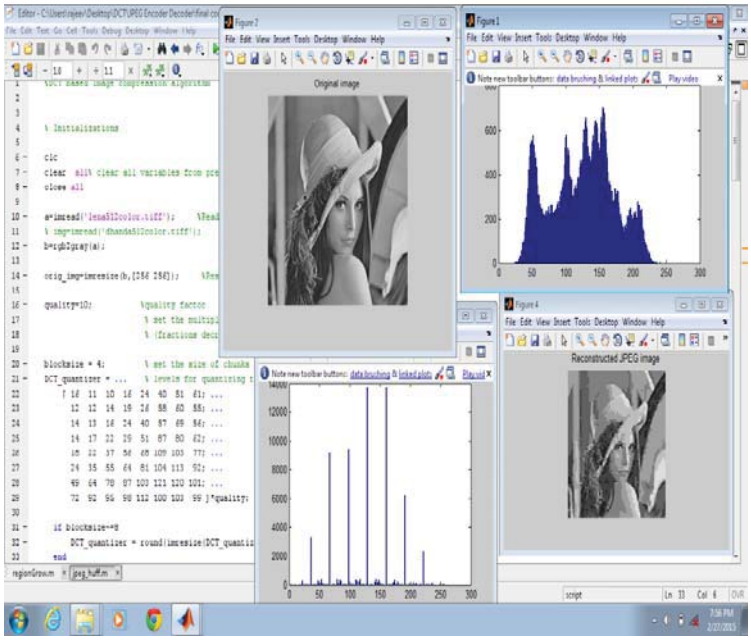

Fig.3 JPEG image compression with quality factor 10

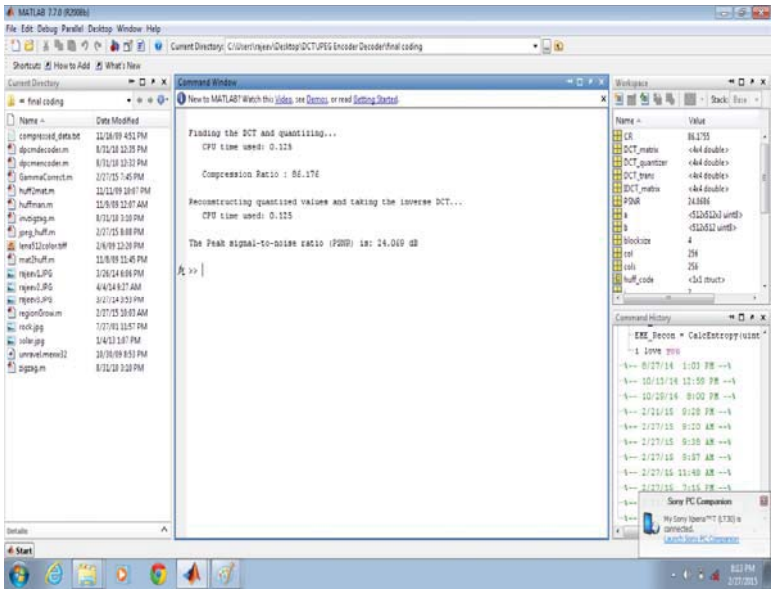

Fig.4 JPEG image compression showing DCT CPU time, Compression ratio PSNR

TABLE I

Sr. No	Quality Factor	CR	DCT /IDCT Processing Time	PSNR (db)
1	6	84.879	0.094/0.078	27.007
2	8	85.498	0.094/0.078	25.953
3	10	85.876	0.125/0.109	24.678
4	12	86.176	0.125/0.125	24.069

Gamma Correction Result:

In this we take the different gamma factor and corresponding result are shown in figure.

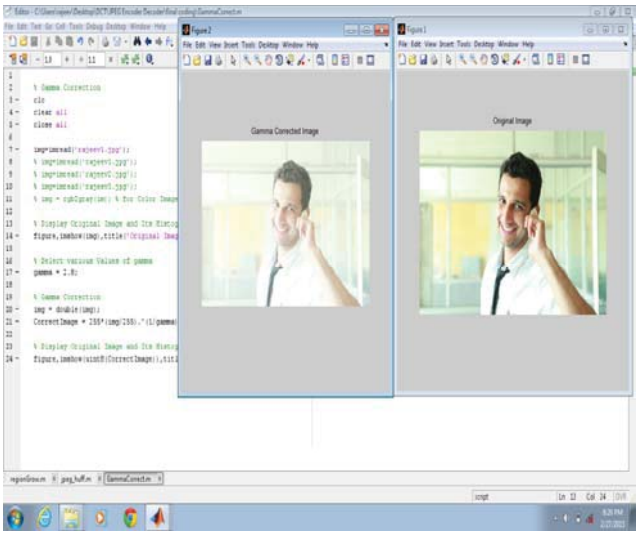

Fig.5 Gamma correction image with gamma factor 2.8

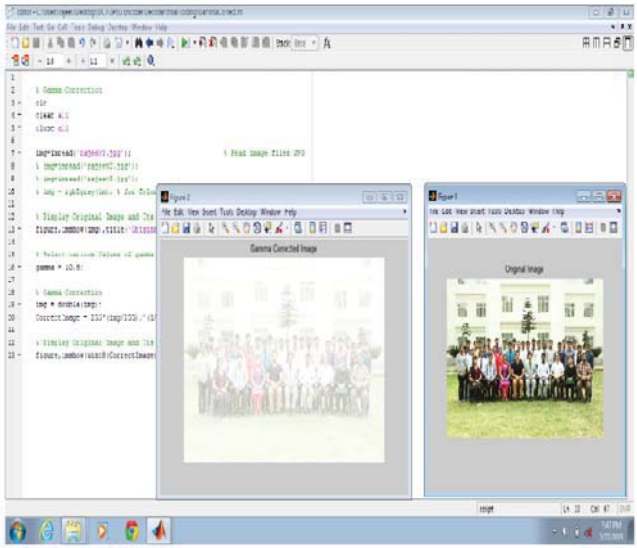

Fig.6 Gamma correction image with gamma factor 10.8

Region Growing:

As shown in figure 7 after applying advanced algorithm we get output result and it can be accomplished by double click on the dark circle of figure 7

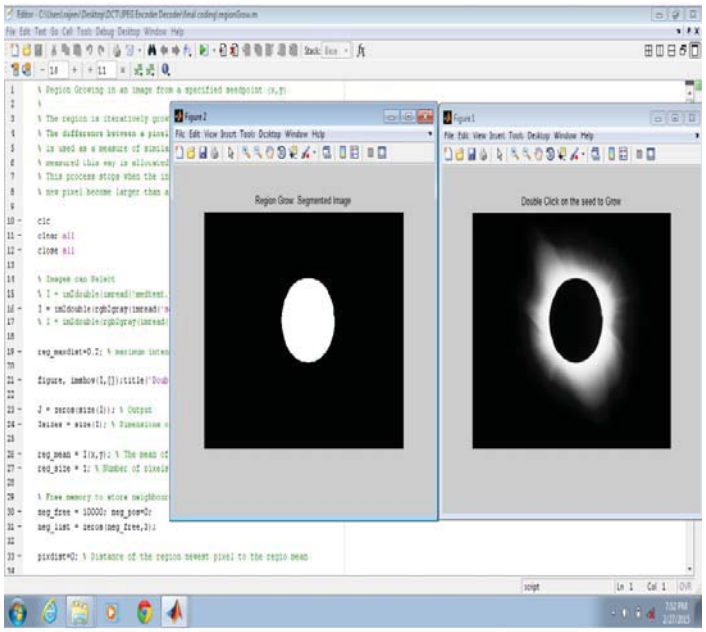

Fig.7 Region growing of an image

V. CONCLUSION

We have made following conclusion: The compression gain can be improved with the increasing scaling factor of original Quantization table. Peak signal to noise ratio varies inversely to the compression ratio. Higher compressed images result in poorer image quality. Mean square error between original and compressed image increase as the scaling factor of original quantization table increases. Discrete cosine transform (DCT) CPU processing time differ from Inverse discrete cosine transform [IDCT]

REFERENCES

[1] Rafael C. Gonzalez," *Digital Image Processing using MATLAB*", 2-e, Pearson Education, 2004.
[2] Gregory K. Wallace, "*The JPEG still picture compression standard*", IEEE Transactions on Consumer Electronics, Vol. 38, No. I, pp. 18-36, February 1992.
[3] Ravi Prakash et.all, "*Enhanced JPEG Compression of Documents*",IEEE International conference of Image Processing, Vol.3,pp.494-497,2001.
[4] ZiqiangCheng,Kee-Young Yoo,"*A Reversible JPEG-to-JPEG Data Hiding Technique*', Fourth International Conference on Innovative Computing, Information and Control pp. 635-639,2009.
[5] Weiqi Luo," JPEG *Error Analysis and Its Applications to Digital Image Forensics*" IEEE Transactions On Information Forensics And Security, VOL. 5, NO. 3, September 2010.
[6] Wei Zheng, ZhisongHou,"*Analysis of JPEG Encoder for Image Compression*" Multimedia Technology (ICMT), International Conference on Digital Object Identifier,pp.205-208, 2011.
[7] S. V. Viraktamathand G. V. Attimarad ,"*Performance Analysis of JPEG Algorithm*", Proceedings of IEEE Conference on Signal Processing, Communication, Computing and Networking Technologies, pp. 628-633, 2011.
[8] XiHongZhou ,"*Research on DCT -based Image Compression Quality*", IEEE Conference Cross Strait Quad-Regional Radio Science and Wireless Technology, pp. 1490-1495, 2011.
[9] HUANGet al. "*Detecting Double JPEG Compression with the Same Quantization Matrix*", IEEE on Information Forensics and Security, VOL. 5, NO. 4, pp. 848-857, Dec., 2011.
[10] Jing-Ming Guo, et.all,"*Secret Communication Using JPEG Double Compression*", IEEE Signal Processing Letters, VOL. 17, NO. 10,pp. 879-883, October 2010.

Design and Implementation of high speed and low power Finite Impulse Response Filter

Deepakshi
Department of Electronics and Communication Engineering
SVIET, Ramnagar,Banur, Punjab, India

Ashish
Department of Electronics and Communication Engineering
SVIET, Ramnagar,Banur, Punjab, India

Abstract- The FIR filters are extensively used in digital signal processing and can be implemented using programmable digital processors. With the advancement in Very Large Scale Integration (VLSI) technology as the DSP has become increasingly popular over the years, the high speed realization of FIR filters with less power consumption has become much more demanding. Since the complexity of implementation grows with the filter order and the precision of computation, real-time realization of these filters with desired level of accuracy is now becoming a challenging task. So, the implementation of FIR filters on FPGAs is the need of the day because FPGAs can give enhanced speed and allows reconfigurable architectures for realization of FIR filter. This is due to the fact that the hardware implementation of a lot of multipliers can be done on FPGA which are limited in case of programmable digital processors.

Keywords – FDA Tool, FIR filter, FPGA,VHDL.

I. INTRODUCTION

A filter is used to remove some component or modify some characteristic of a signal, but often the two terms are used interchangeably. A filter is a device or process that removes some unwanted component or feature from a signal [1].

A finite impulse response (FIR) filter[2] performs a weighted average of a finite number of samples of the input sequence. The basic input-output structure of the FIR filter is a time-domain computation based on a feed-forward difference equation. Figure 1. shows a flow diagram of a standard 3-tap FIR filter.

The filter has seven data registers. The FIR is often termed a transversal filter since the input data transverses through the data registers in shift register fashion. The output of each register (D1 to D2) is called a tap and is termed x[n], where n is the tap number. Each tap is multiplied by a coefficient ck and the resulting products are summed. A general expression for the FIR filters output can be derived in terms of the impulse response. Since the filter coefficients are identical to the impulse response values, the general form of a standard FIR filter can be represented as the following equation

$$y[n] = \sum_{k=0}^{M} h[k]x[n-k]$$

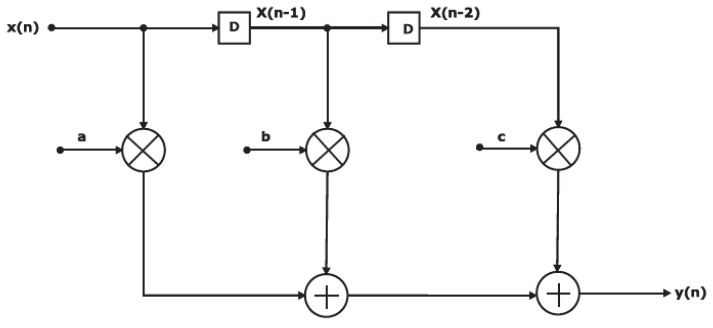

Figure1. FIR filter

When the relation between the input and the output of the FIR filter is expressed in terms of the input and the impulse response, it is called a finite convolution sum. We say that the output is obtained by convolving the sequences x[n] and h[n]. There is a simple interpretation that leads to a better algorithm for achieving convolution. This algorithm can be implemented using the tableau that tracks the relative position of the signal values. The determination of filter coefficients controls the characteristic of the FIR filter.

The output y(n) of a non-recursive filter is a function only of the input signal x(n). The response of such a filter to an impulse consists of a finite sequence of M+ 1 sample, where M is the filter order. Hence, the filter is known as a Finite-Duration Impulse Response (FIR) filter. Other names for a non-recursive filter include all-zero filter, feed-forward filter or moving average (MA) filter a term usually used in statistical signal processing literature.

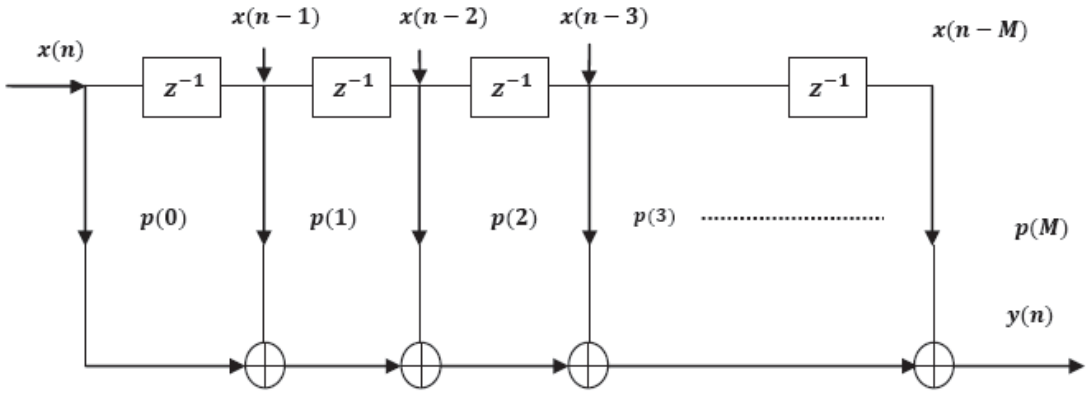

Figure2. Finite Impulse Response Filter Realization

The basic characteristics of Finite Impulse Response (FIR) filters are:

a) Linear phase characteristic

b) High filter order (more complex circuits)

c) Stability

II. LITERATURE REVIEW

Xiaoyan Jiang et al. [3] in introduced structure characteristics and the basic principles of the finite impulse response (FIR) digital filter, and gives an efficient FIR filter design based on FPGA in this paper. Use MATLAB FDATool to determine filter coefficients, and designed a 16-order constant coefficient FIR filter by VHDL language, take use of QuartuslI to simulate filters, the results meet performance requirements.

Kavita et al. [4] presented an efficient design of Modified Booth Multiplier and then also implemented it in this paper. The Modified Booth Recoding method is widely used to generate the partial products for implementation of large parallel multipliers, which adopts the parallel encoding scheme. In this paper the software design of the Modified Booth Multiplier is explained with the help of flow chart. The simulation is done using Xilinx ISE Design Suite 14.2 tool and ModelSim tool and the results obtained are shown both for 4 bit and 8 bit multiplication. The implementation of this multiplier is done using VHDL on Spartan 3E kit and the hardware results are also shown.

Vaidyanathan [5] addressed the use of architectural transformations techniques for the low power realization of FIR filters on dedicated architectures. They experiment a new encoding for the operators, called Hybrid encoding, which is a compromise between the minimal input dependency offered by the binary encoding and the low switching characteristic of the gray encoding. The results shows that with the use of Hybrid operators in FIR architectures power savings of up to 25% are possible, together with 14% delay improvement, and an area penalty of 28%. They implemented dedicated architectures for FIR filters. Arithmetic operators that operate with a different code, the Hybrid encoding, were experimented in the FIR filter architectures. Performance comparisons for pipelined architectures using Binary and Hybrid operators were investigated and the results showed that despite higher area shown by the architectures with Hybrid operators, these architectures can present less minimum clock period and energy per sample. Thus they explored different values for the size of the groups that work as gray codes in the Hybrid encoding scheme reduction by application of these operators in the FIR architectures.

Lu [6] proposed a method for the design of FIR digital filters with low power consumption. In this method, the digital filter was implemented as a cascade arrangement of low order sections. The first section was designed through optimization, then fixed and a second section was added, which was designed so that the first two sections a cascade satisfy again as far as possible the overall required specifications. The process was repeated until as multi-section

filter is obtained that would satisfy the required specifications under the most critical circumstances imposed by the application at hand. In multisection filters of this type, the minimum number of sections required to process the current input signal can be switched in through the use of a simple adaptation mechanism and in this way, the power consumption can be minimized.

III. Experiment and Result

In this paper, the band-pass filter has been designed using Hamming window. The filter specifications are real world and MATLAB FDATOOL is used to find out the filter coefficients. The design of parallel pipelined FIR filter using the encoding scheme – Radix-16 has been accomplished via Hardware Description Language and synthesized on XILINX ISE Software (Xilinx ISE 12.4 version).The circuit diagram of band pass FIR filter is shown in figure 3.

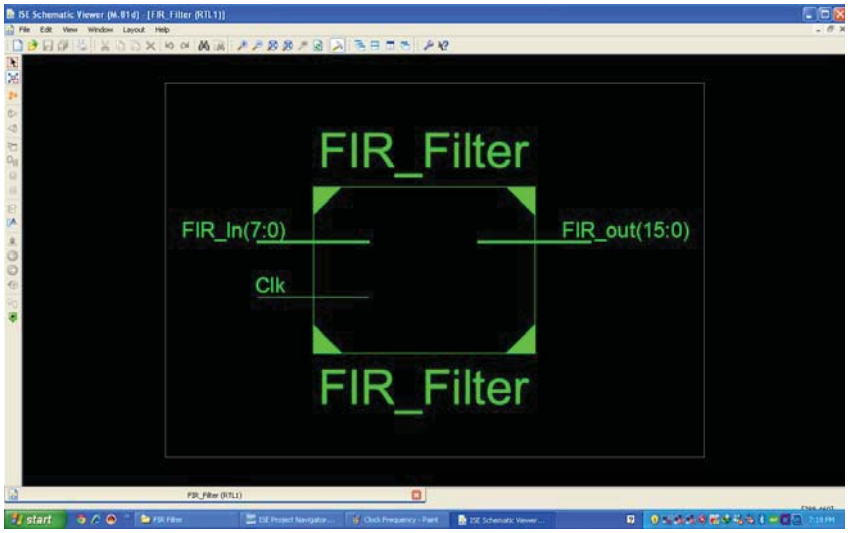

Figure 3. Circuit Diagram of Band-pass Filter

Synthesis results of FIR filter using radix-16 booth multiplier I shown in figure 4.

Module Name:	FIR_Filter	**Implementation State:**	Synthesized
Target Device:	xc6vlx75t-2ff484	**•Errors:**	No Errors
Product Version:	ISE 12.4	**•Warnings:**	2 Warnings (0 new)
Design Goal:	Balanced	**•Routing Results:**	
Design Strategy:	Xilinx Default (unlocked)	**•Timing Constraints:**	
Environment:	System Settings	**•Final Timing Score:**	

Device Utilization Summary (estimated values)			
Logic Utilization	**Used**	**Available**	**Utilization**
Number of Slice Registers	254	93120	
Number of Slice LUTs	608	46560	
Number of fully used LUT-FF pairs	16	846	
Number of bonded IOBs	25	240	
Number of BUFG/BUFGCTRLs	1	32	

Figure 4. Synthesis Report of Pipelined FIR Filter Using Radix-16 Multiplier

Advanced HDL Synthesis Report of parallel pipelined FIR Filter Using Radix-16 Multiplier is shown in figure 5.

```
---------------
Speed Grade: -2

   Minimum period: 1.425ns (Maximum Frequency: 701.681MHz)
   Minimum input arrival time before clock: 4.943ns
   Maximum output required time after clock: 0.659ns
   Maximum combinational path delay: No path found

=========================================================================

Process "Synthesize - XST" completed successfully
```

Figure 5. Advanced HDL Synthesis Report pipelined FIR Filter Using Radix-16 Multiplier

IV.CONCLUSION

In this paper, a band pass FIR filter has been designed using Hamming window. The parallel pipelined form structure is used in designing of this filter as this approach gives better performance than common structures in terms of speed of operation, cost and power consumption. The concept of pipelining has been incorporated that results in reducing the delay of the FIR filter, thereby enhancing the speed and reducing the power dissipation as compared to the non-pipelined techniques. The design of pipelined FIR filter using the encoding schemes Radix-16 are carried out via Hardware Description Language. Simulation and synthesis for FPGAs are accomplished on XILINX ISE Software (Xilinx ISE 12.4 version).

REFERENCES

[1] S. K. Mitra, “Digital Signal Processing”, New York: Tata McGraw Hill, 2005.

[2] S. W. Smith, “The Scientist and Engineer's Guide to Digital Signal Processing”, San Diego: California Technical Publications, 1997.

[3] X. Jiang, and Y. Bao, “FIR filter design based on FPGA”, International Conference on Computer Application and System Modeling, pp. 621-624, 2010.

[4] Kavita and Jasbir Kaur, “Design and Implementation of an Efficient Modified Booth Multiplier using VHDL”, Proceedings of 2nd International Conference on Emerging Trends in Engineering and Management, ICETEM 2013.

[5] P. P. Vaidyanathan, “Optimal Design of Linear-Phase FIR Digital Filters with Very Flat Passbands and Equiripple Stopbands”, IEEE Transactions on Circuits and Systems, vol. 32, no. 9, pp. 904-917, Sep. 1985.

[6] W. S. Lu, A. Antoniou, and S. Saab, “Sequential design of FIR digital filters for low power DSP applications”, Conference Record of the Thirty-First Asilomar Conference on Signals, Systems &amp, IEEE, pp. 701-704, 1997.